Please cite as: Stukel, M. R., Decima, M., Selph, K. E., Gutierrez-Rodriguez, A. (2021). Size-specific grazing and competitive interactions between large salps and protistan grazers. Limnology and Oceanography. doi: 10.1002/lno.11770

Size-specific grazing and competitive interactions between large salps and protistan grazers

Michael R. Stukel[1,2,*], Moira Décima[3,4], Karen Selph[5], Andres Gutiérrez-Rodríguez[3]

[1]Dept. of Earth, Ocean, and Atmospheric Science, Florida State University, Tallahassee, FL
[2]Center for Ocean-Atmospheric Prediction Studies, Florida State University, Tallahassee, FL
[3]National Institute of Water and Atmospheric Research (NIWA), Wellington, New Zealand
[4]Scripps Institution of Oceanography, University of California San Diego, SA
[5]Dept. of Oceanography, University of Hawaii at Manoa, Honolulu, HI
[*]Corresponding Author: mstukel@fsu.edu

Keywords: zooplankton, pelagic tunicates, plankton ecology, protozoans, mesozooplankton, filter feeding, grazing rates, microzooplankton, bacterioplankton, cyanobacteria, euphausiids, *Euphausia superba*

Abstract

We investigated competition between *Salpa thompsoni* and protistan grazers during Lagrangian experiments near the Subtropical Front in the southwest Pacific sector of the Southern Ocean. Over a month, the salp community shifted from dominance by large (>100-mm) oozooids and small (<20-mm) blastozooids to large (~60-mm) blastozooids. Phytoplankton biomass was consistently dominated by nano- and microphytoplankton (>2 µm cells). Using bead-calibrated flow-cytometry light scatter to estimate phytoplankton size, we quantified size-specific salp and protistan zooplankton grazing pressure. Salps were able to feed at a >10,000:1 predator:prey size (linear-dimension) ratio. Small blastozooids efficiently retained cells >1.4-µm (high end of picoplankton size, 0.6-2 µm cells) and also obtained substantial nutrition from smaller bacteria-sized cells. Larger salps could only feed efficiently on >5.9-µm cells and were largely incapable of feeding on picoplankton. Due to the high biomass of nano- and microphytoplankton, however, all salps derived most of their (phytoplankton-based) nutrition from these larger autotrophs. Phagotrophic protists were the dominant competitors for these prey items and consumed approximately 50% of the biomass of all phytoplankton size classes each day. Using a Bayesian statistical framework, we developed an allometric-scaling equation for salp clearance rates as a function of salp and prey size:

$$Clearance(ESD) = \varphi \cdot TL^{\psi} \times \min\left(\frac{\left(ESD/_{\theta \times TL}\right)^2}{0.16+\left(ESD/_{\theta \times TL}\right)^2}, 1\right) \times Q_{10}^{(T-12°C)/10}$$

where ESD is prey equivalent spherical diameter, TL is *Salpa thompsoni* total length, $\varphi = 5.6\times10^{-3} \pm 3.6\times10^{-4}$, $\psi = 2.1 \pm 0.13$, $\theta = 0.58 \pm 0.08$, and $\gamma = 0.46 \pm 0.03$. We discuss the biogeochemical and food-web implications of competitive interactions between salps, krill, and protozoans.

Introduction

Salps play a unique ecological and biogeochemical role as large, gelatinous grazers that can feed rapidly and efficiently on some of the smallest phytoplankton in the ocean (Kremer and Madin 1992; Bone 1998; Sutherland et al. 2010). Indeed, salps can feed at one of the highest predator:prey size ratios (>10,000:1) of any organism in the ocean (Kremer and Madin 1992; Fuchs and Franks 2010). Their rapidly-beating muscle bands also allow them to routinely filter >1000 times their biovolume per hour (Harbison and Gilmer 1976; Madin et al. 2006). By compacting microscopic prey into very large, rapidly-sinking fecal pellets, their blooms can reshape pelagic biogeochemical pathways and increase CO_2 sequestration in the deep ocean (Bruland and Silver 1981; Madin 1982). However, as a result of their patchy distributions, poor preservation during typical net tows, and difficulties associated with experimental work with gelatinous taxa, they remain understudied (Henschke et al. 2016).

Traditionally, and especially in the Southern Ocean, salps have been considered competitors of crustaceans, especially the Antarctic krill, *Euphausia superba* (Loeb et al. 1997; Pakhomov et al. 2002). The assumption of competitive interactions between these groups is driven, in part, by their roughly similar sizes and collection by the same methodology (net tows). However, *E. superba* feed preferentially on large diatoms (Haberman et al. 2003), while salps are largely non-selective feeders that can efficiently consume all nano- and microphytoplankton, and less efficiently consume picophytoplankton (Kremer and Madin 1992; Sutherland et al. 2010). Salps also have distinctly different life cycles than crustaceans. Their alternation of generations, featuring solitary asexual oozooid phases and chain-forming sexual blastozooids, allows rapid population growth on time scales of days to weeks in warm temperatures and weeks to months in the Southern Ocean (Bone 1998; Lüskow et al. 2020). In contrast, *E. superba* has a multi-year life cycle, with population fluctuations linked to interannual climate variability (Pakhomov 2000; Saba et al. 2014).

Given these considerations, we ask whether phagotrophic protists may potentially be more important competitors of salps. Phagotrophic protists (heterotrophs and mixotrophs) are taxonomically diverse and the dominant grazers of picoplankton (Sherr and Sherr 1994; Caron et al. 2012). They also consume from 59 to 75% of all phytoplankton production across diverse marine ecosystems, including in some of the coldest waters near the Antarctic continent (Calbet and Landry 2004; Garzio et al. 2013). These grazers have rapid growth rates, potentially higher than a doubling per day at tropical temperatures, and higher than a doubling per week even at the coldest temperatures in the Southern Ocean (Hansen et al. 1997). Considering these similarities in prey and growth rates, phagotrophic protists are likely more important as competitors of salps than crustaceans, although the consumers of salps and protists are likely very different. Bacterivorous and herbivorous protists are themselves important prey for other phagotrophic protists and play a significant role in supporting metazoan zooplankton in many ecosystems (Calbet 2008; Landry et al. 2020). With sizes (linear dimension) two to four orders of magnitude greater than protists, however, salps are primarily consumed by either nekton or specialized crustacean micro-predators, including hyperiid amphipods (Madin and Harbison 1977; Henschke et al. 2016).

To test the hypothesis that salps and protistan grazers compete for prey, we conducted a series of protistan and salp grazing experiments during Lagrangian studies conducted near the Chatham Rise in water parcels with blooms of *Salpa thompsoni*. The Chatham Rise is a topographic feature that extends 1000 km east of New Zealand. This region is characterized by strong latitudinal gradients with the Subtropical front (STF) separating warmer, N-limited subtropical waters to the north from colder, Fe-limited subantarctic waters. The co-location of the STF with this topographic feature leads to increased mixing and productivity (Sutton 2001; Chiswell et al. 2013). Most of this primary productivity is consumed by protistan zooplankton, and these protists in turn serve as important components of crustacean diets (Zeldis and Décima 2020). Previous studies have also shown the common presence of salp swarms in the region (Bradford 1985; Zeldis et al. 1995), allowing us to conduct experiments to target salp and protist interactions. We assessed the in situ size spectra of phytoplankton and quantified size-specific grazing rates of both protists and *S. thompsoni*. Our results show that *S. thompsoni* efficiently consumes most nano- and microphytoplankton, and their small blastozooids also feed on picophytoplankton. However, *S. thompsoni* blastozooids and oozooids derived the majority of their nutrition from nano- and microphytoplankton. Phagotrophic protists were the dominant predators on all size classes of phytoplankton, highlighting their importance as competitors of salps, although salps can also efficiently consume these phagotrophic protists.

Methods

Cruise design – We used a Lagrangian process study design to conduct detailed investigations of salp and protist grazing pressure near the Chatham Rise in November, 2018 during the Salp Particle expOrt and Oceanic Production (SalpPOOP) expedition on board the RV *Tangaroa*. We used information from historical zooplankton sampling in the region and the distributions of fish taxa that prey on salps to identify regions with high likelihood of salp presence. We then conducted an areal survey with ~hourly net tows to identify water parcels with high salp abundance and used Lagrangian drift arrays to track these water parcels

Please cite as: Stukel, M. R., Decima, M., Selph, K. E., Gutierrez-Rodriguez, A. (2021). Size-specific grazing and competitive interactions between large salps and protistan grazers. Limnology and Oceanography. doi: 10.1002/lno.11770

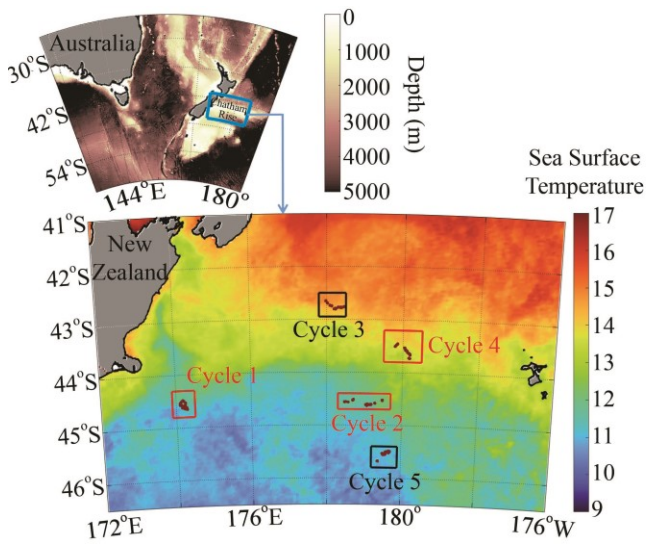

Figure 1 – Study region. Upper plot shows bathymetry of the broader oceanographic region. Lower plot shows our study area with monthly-average SST (NASA MODIS satellite). Net tow locations are indicated with red dots. Red rectangles indicate locations of +Salp Lagrangian cycles. Black squares represent locations of cycles with few or no salps.

while conducting detailed investigation of the evolving plankton community over periods ranging from 4 - 8 days (hereafter referred to as Lagrangian "cycles"). One Lagrangian drift array (which we refer to as the "incubation array") consisted of a satellite-enabled surface float, a 3×1-m holey-sock drogue centered at 15-m depth in the mixed layer, and metal loops at 18 depths allowing us to affix mesh bags containing experimental bottles to be incubated in situ (Landry et al. 2009). We conducted three Lagrangian experiments (hereafter referred to as "cycles") in waters with salps and focus on these results here, although two additional cycles were conducted in non-salp waters (Fig. 1).

During each cycle, we collected samples for phytoplankton analyses from daily CTD casts at ~02:00 local time. Samples included flow cytometry and size-fractionated chlorophyll *a* (Chl *a*) (<2 µm, 2-20 µm, >20 µm) at 6 depths. We sampled from the same depths and casts for daily 24-h incubations, using the two-point dilution technique (Landry et al. 1984) coupled to flow-cytometry analysis to quantify size-specific protistan grazing rates *in situ*. We also conducted twice daily oblique bongo net tows (0.71-m diameter, 200-µm mesh) from the surface to 200 m depth at approximately local noon and midnight to quantify salp abundance, size structure, and gut pigment content. A second type of net, which we refer to as a "salp net" (1-m diameter, 200-µm mesh, with a large (30-L) non-filtering polycarbonate cod end), was used to collect salp specimens for experimental work, including incubations to quantify salp grazing pressure. For detailed information, see online supplementary methods 1.

Salp abundance and biomass estimation - Zooplankton net tows were conducted at least twice daily (day and night) to a depth of 200 m. Salps were sorted, measured for length, identified to species, and staged into oozooid (solitary) or blastozooid (aggregate). A subsample from each tow was taken for determination of Chl *a* in salp guts. *S. thompsoni* total lengths were divided into 5-mm bins (5- to 140-mm) from which we computed normalized abundance size spectra (NASS = salp abundance within a bin divided by bin width).

Protistan grazing experiments – We conducted daily two-point in situ protistan grazing dilution experiments at 6 depths in the water column (Landry et al. 1984; Landry et al. 2009). A control bottle and a "dilute" treatment bottle (25% whole seawater:75% 0.1-µm filtered seawater) were incubated in situ on the drifting array for 24 h. Initial and final samples were taken for flow cytometry and Chl *a* analyses. Daily specific mortality rates due to protistan grazing were calculated as: $m = (k_{dil}-k_{whole})/(1-dil)$, where k_{dil} is the growth rate in the diluted treatment bottle, k_{whole} is the growth rate in the control bottle, and dil is the fraction of whole seawater in the dilute treatment bottle (25%).

Salp grazing experiments – To determine the size-specificity of salp grazing, we conducted grazing incubations in 20-L plankton kreisels or 30-L pseudo-kreisels filled with mixed layer seawater. Salps were collected via short, slow tows through the mixed layer with the salp net. Healthy specimens were transferred into one of the paired kreisels, while the second kreisel was used as a control treatment. We incubated *S. thompsoni* blastozooids and oozooids ranging in size from 50 – 128 mm total length. We also conducted three incubations with a chain of blastozooids (6 – 8 mm individuals) released by an oozooid inside of one of the plankton kreisels. We found that this was the only way to successfully obtain such small blastozooids in healthy conditions. Incubations typically lasted ~24 h and were sampled every ~2 h for flow cytometry.

Gut pigment measurements – Because previous studies have shown that salp filtration rates can be underestimated when salps are incubated in a tank (Pakhomov et al. 2002), we also collected organisms for gut pigment analysis from bongo tows conducted multiple times daily (Madin and Cetta 1984). Chl *a* and phaeopigment content (together GPig, units = µg Chl *a* equivalents $salp^{-1}$) in excised guts was measured using the acidification method (Strickland and Parsons 1972; Décima et al. 2019). We estimated gut pigment turnover (GPT) time using the following equation GPT(h) = 2.607×ln(OAL, mm) - 2.6. Chlorophyll-based grazing was estimated as: G (µg Chl *a* equiv. $salp^{-1}$ h^{-1}) = Gpig×GPT^{-1}.

Flow cytometry – Flow cytometry samples from the water column, protistan grazing dilution experiments, and salp incubations were analyzed at sea to estimate the abundance and size of eukaryotic phytoplankton. Cell diameter was estimated from forward light scatter calibrated with polystyrene beads. Biomass was estimated from diameter using equations in Menden-Deuer and Lessard (2000).

Size-specific grazing rate calculations – From flow cytometry samples in salp and protistan grazing rate experiments, we calculated normalized biomass size spectra (NBSS) for eukaryotic phytoplankton from 0.8 - 31 µm. We calculated the normalized biomass as:

$$B_n(ESD) = \sum_{\frac{ESD}{2}}^{2\times ESD} Biomass/(2 \times ESD - ESD/2) \quad \text{Eq. 1}$$

Phytoplankton mortality due to protistan grazing as a function of size was computed from initial and final NBSS for each experiment. To determine an average grazing rate for each Lagrangian cycle, we averaged all grazing rate estimates, m(ESD), made in the mixed layer during that cycle. We used results from these in situ protistan grazing experiments to compute protistan grazing rate-corrected size-specific mortality of phytoplankton due to salp grazing in our on-deck incubations (G, units of d^{-1}) as:

$$G(ESD) = \frac{m(ESD)\left(\left(\frac{vol}{f_i N}\right)\left(e^{-\frac{f_i \times N}{vol}t}-1\right)+t\right)-\ln\left(\frac{B_{n,t}(ESD,t)}{B_{n,c}(ESD,t)}\right)}{t} \quad \text{Eq. 2}$$

where $B_{n,c}$ is the normalized biomass in the control kreisel at time t, $B_{n,t}$ is the normalized biomass in the treatment kreisel (with salps) at time t, vol is the volume of the kreisel, N is the number of salps in the treatment kreisel, and f_i is an initial estimate of salp filtration rate. Throughout this manuscript we use the term 'filtration rate' to refer to the volume of water pumped through a salp per unit time (which is independent of prey cell size), while we use the term 'clearance rate' to refer to the volume of water cleared by salps of a particular prey size per unit time. Clearance rate is thus less than or equal to filtration rate and varies for differently sized prey. G(ESD) relates to the actual clearance rate of the salps (C, units of L $salp^{-1}$ d^{-1}) through the equation: C(ESD)=G(ESD)/N/vol. For derivation of Eq. 2, see Supp. Methods 3. For additional details on all field methods, see Supp. Methods 1.

Bayesian parameter estimation and model selection – For every salp incubation, we calculated clearance rate as a function of prey ESD using two simple models. The first assumes clearance rates depend only on the filtration rate and filter mesh of the salp and uses a two-parameter function in which F is the filtration rate of the salp and τ is a parameter that is approximately equal to the equivalent mesh size of the salp:

$$Clearance(ESD) = \min\left(\frac{(ESD/\tau)^2}{0.16+(ESD/\tau)^2}, 1\right) \times F \quad \text{Eq. 3}$$

The second equation is a three-parameter model that adds a functional form representing potential escape responses of prey, assuming that prey swimming velocity is proportional to size:

$$Clearance(ESD) = \min\left(\frac{(ESD/\tau)^2}{0.16+(ESD/\tau)^2}, 1\right) \times e^{-\lambda \cdot ESD} \times F \quad \text{Eq. 4}$$

where λ is a parameter that describes the evasion success of prey. Derivation of these equations is given in Supp. Methods 4. To fit these parameters to the

incubation data, we used a Bayesian statistical framework (see Supp. Methods 2). To objectively choose whether Eq. 3 or 4 was more appropriate for each incubation, we used deviance information criterion (DIC, Spiegelhalter et al. 2002).

To quantify the salp-size-dependence of filtration rate and equivalent mesh size, we also fit allometric-scaling relationships to the data from all incubations:

$$Clearance(ESD) = \varphi \times TL^{\psi} \times \min\left(\frac{\left(ESD/_{\theta \times TL^{\gamma}}\right)^2}{0.16+\left(ESD/_{\theta \times TL^{\gamma}}\right)}, 1\right) \times Q_{10}{}^{(T-12°C)/10} \quad \text{Eq. 5}$$

$$Clearance(ESD) = \varphi \times TL^{\psi} \times \min\left(\frac{\left(ESD/_{\tau}\right)^2}{0.16+\left(ESD/_{\tau}\right)}, 1\right) \times Q_{10}{}^{(T-12°C)/10} \quad \text{Eq. 6}$$

Where TL is salp total length, $\varphi \times TL^{\psi}$ is an allometric-scaling relationship for the filtration rate, $\theta \times TL^{\gamma}$ is an allometric-scaling relationship for τ (equivalent mesh diameter), T is temperature, and Q_{10} is a temperature scaling factor that we assume is equal to 2 (Madin and Purcell 1992). Eq. 6 assumes that τ does not vary with salp size. We again chose between the two equations based on DIC.

Because salp filtration rates are often lower in incubations than in situ (Pakhomov et al. 2002), we also fit Eq. 5 (which was found to be a better predictor than Eq. 6) to gut pigment data results. For this analysis, we combined in situ mixed layer carbon-based NBSS with mixed layer size-fractionated Chl *a* measurements to determine in situ Chl *a*-based NBSS. We then fit Eq. 5 to the results of Chl *a*-based consumption rates (mg Chl *a* h^{-1}) determined from gut pigment measurements.

Results

Environmental conditions and salp abundances – We found salps in three water parcels in the vicinity of the Chatham Rise and the STF (Fig. 1). The highest salp abundance was found in a *S. thompsoni*-dominated coastal region in modified subantarctic water (Cycle 1). Surface Chl *a* was 0.9 µg L^{-1} and surface temperature was 11°C. Cycle 2, conducted further offshore and in subantarctic water along the southern flank of the STF, featured a mixed salp community, with substantial abundances of *S. thompsoni*, but also other abundant taxa including *Pegea confoederata* and *Thetys vagina* (although we only present results from *S. thompsoni* in this manuscript). Surface Chl *a* was substantially lower (0.4 µg L^{-1}) and surface temperature was 10°C. During Cycle 4 we sampled a region of mixed water featuring characteristics representative of subtropical water that had likely experienced mixing with subantarctic water near the STF. Surface temperature on Cycle 4 was ~13°C and surface Chl *a* was 1.3 µg L^{-1}. Heterotrophic bacteria abundance in the surface mixed layer averaged 9.3×10^5, 1.4×10^6, and 2.6×10^6 cells mL^{-1}, in Cycles 1, 2, and 4, respectively. Euphotic zone depths (to 1% of surface irradiance) were relatively shallow at 32, 35, and 25 m for Cycles 1, 2, and 4, respectively, and surface mixed layer depths were 23, 48, and 21 m, respectively.

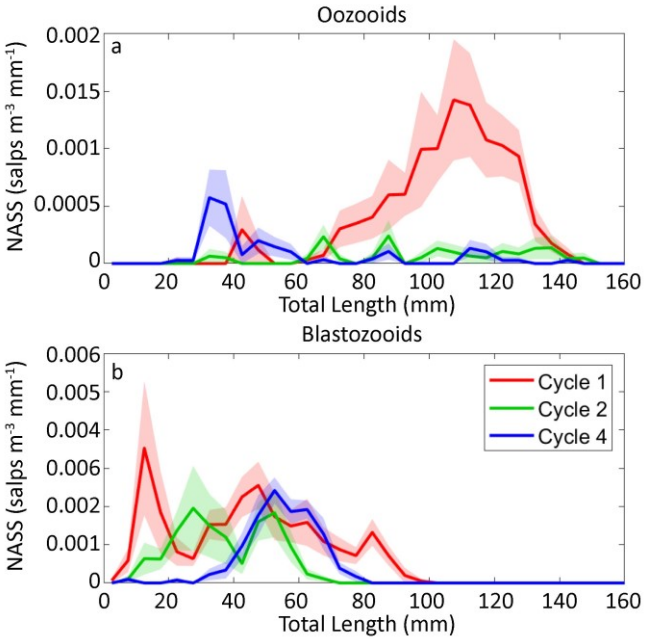

Figure 2 – Normalized abundance size spectra (NASS, salps m^{-3} mm^{-1}) as a function of the length of *Salpa thompsoni* oozooids (a) and blastozooids (b) in each cycle.

We also conducted two cycles in subtropical (Cycle 3) and subantarctic (Cycle 5) waters without salp blooms. Hydrographic properties and phytoplankton abundance during these cycles were largely similar to those encountered during Cycles 4 and 2, respectively.

The size structure of the *S. thompsoni* population varied substantially between cycles (Fig. 2). Cycle 1 was the only cycle with a high abundance of large oozooids (80 to 130 mm), and small (~10 and ~40 mm) blastozoooids were also abundant. Cycle 2, which appeared to represent a temporal progression of the bloom encountered in Cycle 1, was dominated by medium-sized blastozooids (25 – 50 mm), with very few oozooids present. By Cycle 4 (approximately one week

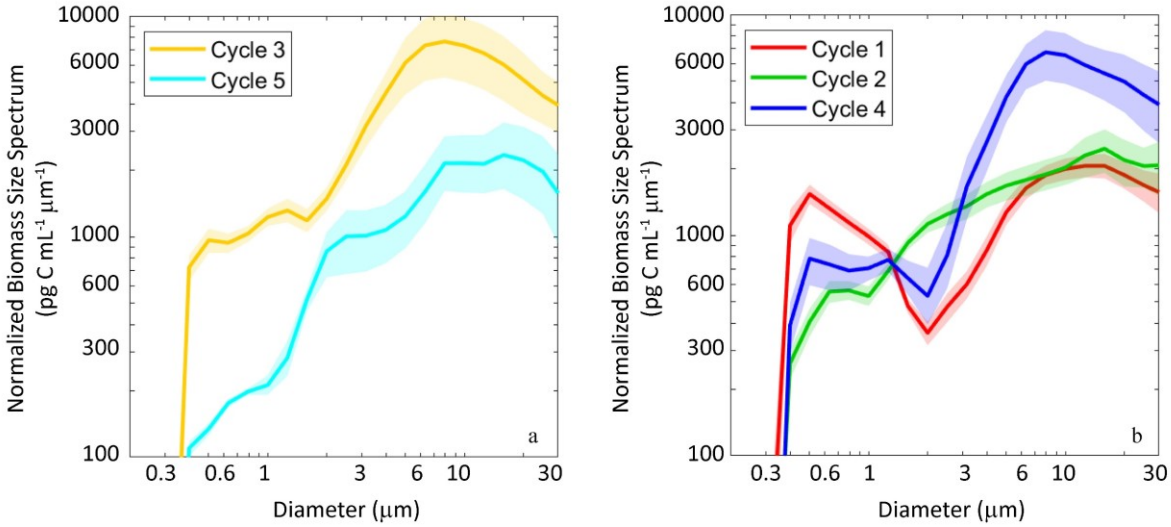

Figure 3 – Normalized biomass size spectra (pg C mL^{-1} μm^{-1}) as a function of prey diameter (µm) of mixed layer eukaryotic phytoplankton communities for non-salp cycles (a) and salp cycles. Shaded areas are 95% confidence intervals.

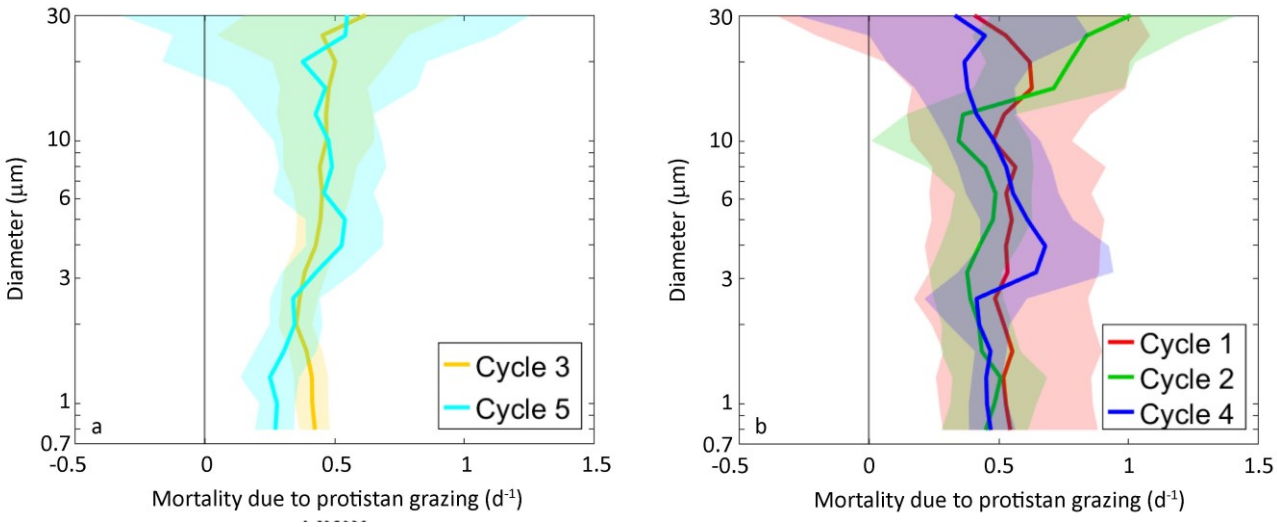

Figure 4 – Phytoplankton mortality due to protistan grazing (d^{-1}) as a function of prey diameter (µm) for non-salp cycles (a) and salp cycles (b). Results are from multiple repeated grazing experiments conducted in situ at multiple depths spanning the mixed layer. Cycle averages are shown in heavier lines, whereas 95% confidence limits are shaded.

later), the salp community was dominated by large blastozooids (50 – 70 mm) and a new generation of small oozooids appeared.

Phytoplankton size spectra and protistan grazing – The phytoplankton normalized biomass size spectrum varied between cycles, although phytoplankton biomass consistently peaked near the upper end of the nanophytoplankton size range (i.e., 7 – 20 µm, Fig. 3). During Cycle 1, the cycle with the highest salp abundance and also the closest to land, there was a substantial abundance of picoeukaryotic phytoplankton (0.5 – 1 µm), comparatively few phytoplankton with an ESD of ~2 µm, and a greater biomass of 5 – 30 µm phytoplankton than smaller taxa. During Cycles 2 (salps) and 5 (no salps), which were both conducted in water of primarily subantarctic origin, there were fewer picoeukaryotic phytoplankton and carbon biomass increased nearly monotonically with size from picophytoplankton to a peak at ~15 µm ESD. Cycles 3 (no salps) and 4 (salps) in subtropical water featured fairly consistently low biomass of phytoplankton from 0.5 – 3.0 µm, followed by a rapid increase in biomass with increasing size to a peak at ~8 µm.

Across cycles and size classes, protists consumed ~50% of phytoplankton biomass per day (Fig. 4), with some variability between cycles. For instance,

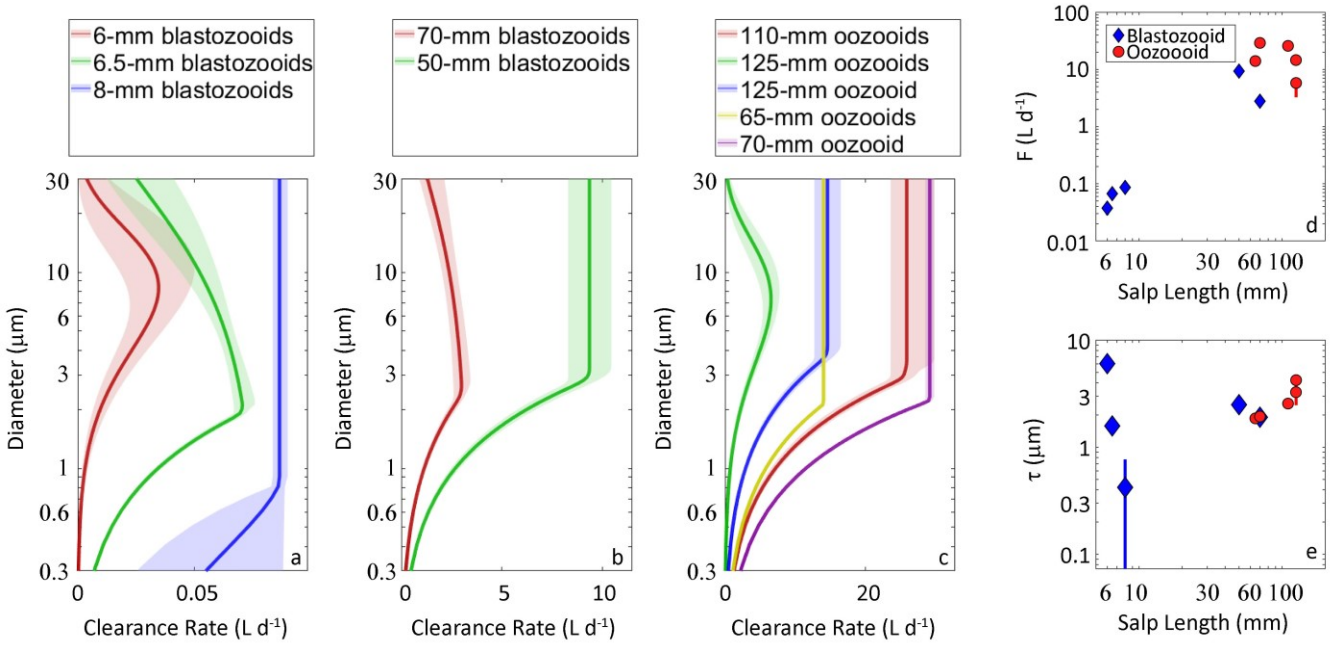

Figure 5 – Salp clearance rates (L $salp^{-1}$ d^{-1}) as a function of prey diameter (µm) estimated from deckboard *Salpa thompsoni* grazing experiments conducted in plankton kreisels: small blastozooids (a), large blastozooids (b), large oozooids (c). Colors indicate different salp incubation experiments. Salp filtration rate (F, L d^{-1}) as a function of total salp length (mm) (d). Effective filter mesh size (τ, µm) as a function of total salp length (mm) (e).

phytoplankton mortality due to protistan grazing was higher for microplankton than for pico- and nanoplankton during Cycle 2, but fairly similar to or slightly lower than mortality of nanoplankton for Cycles 1 and 4. These differences, however, were not statistically significant, and we found no significant difference between protistan grazing rates during non-salp cycles (Fig. 4a) and salp cycles (Fig. 4b). However, we note that uncertainty was substantial for microplankton, because these cells were far less abundant than pico- and nanophytoplankton so their abundance estimates based on small volumes analyzed by flow cytometry are inherently more variable.

Salp grazing incubations – We used a Bayesian statistical framework to combine flow cytometry-derived phytoplankton abundance changes in salp incubations into size-specific estimates of salp clearance rates (Fig. 5). Small blastozooids (Fig. 5a) had maximum clearance rates <0.1 L salp^{-1} d^{-1}. The youngest salps had substantially lower grazing rates than even 3-day old (8-mm) blastozooids. The 8-mm blastozooids fed efficiently even on phytoplankton <1 µm in diameter. Larger blastozooids (Fig. 5b) and oozooids (Fig. 5c) had filtration rates that ranged from 2 – 30 L salp^{-1} d^{-1}, with no clear dependence on their size (Fig. 5d).

The equivalent mesh size (τ), which is essentially the prey size below which clearance rate begins to decrease substantially, was typically 2 – 3 µm (Fig. 5e). However, it was substantially lower for 8-mm blastozooids (0.4 µm). Contrarily, the smallest blastozooids (6-mm) had the largest equivalent mesh size (6 µm), although this newly released chain appeared to be only weakly feeding. Only four of ten incubations showed statistically significant evidence for prey avoidance at large prey sizes, and these experiments contained organisms that were feeding with lower filtration rates than other similarly sized salps. Since previously published evidence suggests that salp filtration rates are higher in situ than in tank experiments, this leads us to believe that prey avoidance behaviors did not significantly reduce filtration rates on the size of prey we assessed (0.7 – 30 µm). This does not, however, suggest that larger prey taxa with stronger swimming behaviors (e.g., crustacean nauplii) cannot successfully avoid capture by salps.

To further investigate allometric grazing relationships, we constrained Eqs. 5 and 6 using all incubation data. The DIC computed after fitting Eq. 5 (which includes allometric scaling of the equivalent mesh size) was lower than for Eq. 6 (3.51×10^4 vs. 3.65×10^4) suggesting that it is a better fit to the data. Parameters fit with this model were: $\varphi = 1.5\times10^{-3} \pm 1.4\times10^{-4}$, $\psi = 2.1 \pm 0.02$, $\theta = 0.55 \pm 0.08$, and $\gamma = 0.45 \pm 0.03$. For perspective, these results suggest that the equivalent mesh size of a salp increases from 1.2 µm for a 6-mm salp to 4.7 µm for a 125-mm salp, while the filtration rate increases from 0.06 to 39.9 L salp^{-1} d^{-1}.

Salp grazing rates in situ – We measured the gut pigment content of 776 salps ranging in length from 6 - 150 mm. This included 521 blastozooids ranging from 9 - 97 mm and 255 oozooids ranging from 21 - 150 mm. These estimates were used to quantify in situ salp grazing rates (µg Chl *a* salp^{-1} d^{-1}), which were combined with size-fractionated Chl *a* measurements from the mixed layer to constrain Eq. 6 using in situ data (Fig. 6). Parameters fit with this model were: $\varphi = 5.6\times10^{-3} \pm 3.6\times10^{-4}$, $\psi = 2.1 \pm 0.13$, $\theta = 0.58 \pm 0.08$, and $\gamma = 0.46 \pm 0.03$. Notably, the value for ψ (exponent of the filtration rate to salp length relationship) was very close to the equivalent parameter determined from incubation results. However, φ (the intercept) was nearly a factor of four greater, suggesting that salp filtration rates were approximately four-times greater in situ than in the plankton kreisels. Using the results of our analysis, we estimate that a 6-mm, newly-released blastozooid filtered 0.24 L salp^{-1} d^{-1}, while a 150-mm oozooid filtered 208 L salp^{-1} d^{-1}. We also estimate that the equivalent mesh spacing (τ) ranged from 1.3 – 5.8 µm.

Eq. 6 and the in situ parameterization allow us to quantify volume-specific salp clearance rates for different prey sizes. As expected, because $\psi < 3$, specific clearance rates decrease with increasing size. The smallest salps assessed in our study (~6-mm) had clearance rates of ~12,000 body volumes per day for prey >1.6 µm. These small salps were fairly efficient at feeding on even smaller prey. For instance, their filtration rate on 0.8-µm cells was ~6,000 body volumes per day. Volume-specific filtration rates were substantially lower for the largest salps collected in our study (150-mm). These salps had clearance rates of ~4,000 body volumes d^{-1} for cells >6 µm, but <300 body volumes d^{-1} for 0.8-µm cells. We caution that these results may potentially underestimate salp clearance rates, because they assume that the salps were actively feeding at the time of collection and that all salps were feeding in the mixed layer, although our net tows went to a depth of 200 m. It is possible that the salps in Fig. 6 with low apparent grazing rates (relative to their size) were actually living beneath the euphotic zone, thus even high clearance rates would yield low gut pigment content.

We then used in situ salp abundances (Fig. 2) to quantify the clearance rates of the entire salp community. Although net tows were made to a depth of 200 m, we assumed in this calculation that all salps were collected in the euphotic zone. While this may overestimate salp abundance in the euphotic zone, it is offset by our previous assumption that all salps were collected in the mixed layer leading to an underestimate of clearance rates. For Cycle 1, with the highest salp abundance,

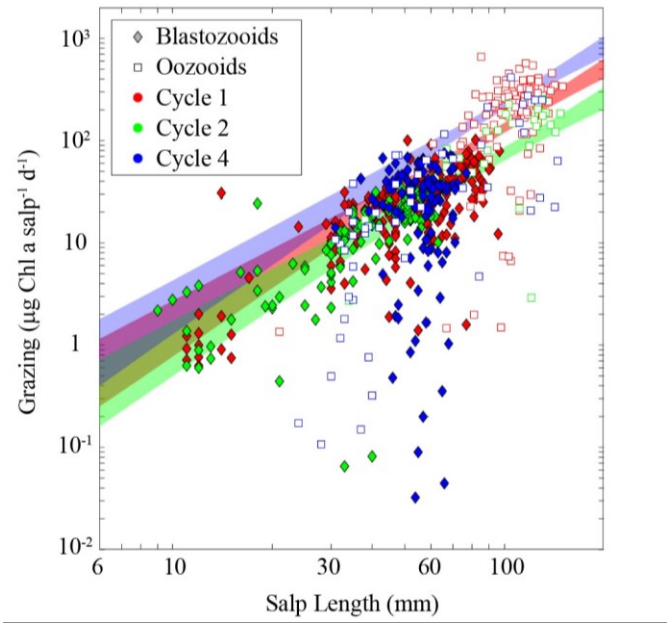

Figure 6 – Salp grazing rates (µg Chl *a* salp^{-1} d^{-1}) as a function of salp length (mm) determined from in situ gut pigment measurements for all cycles and for blastozooids and oozooids. Colored lines show Bayesian estimates of grazing as a function of *Salpa thompsoni* length (accounting for in situ mixed layer temperature and normalized Chl *a* size spectra for each cycle).

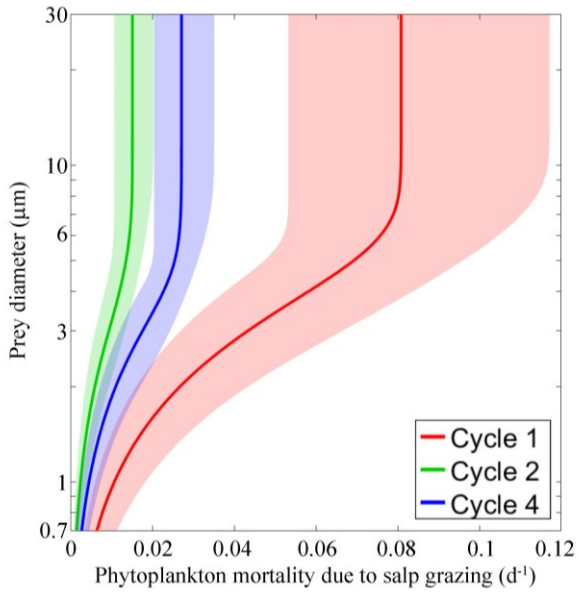

Figure 7 – Phytoplankton mortality (d^{-1}) due to grazing of the *Salpa thompsoni* community as a function of prey diameter (µm) for each cycle. Results are derived from Eq. 6 with in situ parameterization and cycle-specific salp abundance.

salp grazing pressure cleared 8.1% of the biomass of >6-µm phytoplankton each day (Fig. 7). Smaller phytoplankton had lower mortality rates due to salp grazing (4.3% and 1.1% d^{-1} for 3- and 1-µm phytoplankton, respectively). Salp grazing pressure was lower during the other cycles (1.5% d^{-1} for large cells in Cycle 2; 2.7% d^{-1} in Cycle 4).

Because most phytoplankton carbon was contained in >5-µm nano- and microphytoplankton that were efficiently preyed upon by all salp sizes, the median (carbon-weighted) prey size was relatively invariant with salp size. Median prey size was similar at 8-9 µm for salps in all cycles. This shows a ~1,000:1 average predator:prey size ratio (linear dimension) for the smallest blastozooids collected in our study and a >10,000:1 average predator:prey ratio for large oozooids.

Total ingestion was determined primarily by nano- and microphytoplankton prey concentration (which varied between the three cycles) and filtration rate. During Cycles 1 and 2, the smallest salps consumed 4 – 5 µg C from phytoplankton daily, while during Cycle 4 they consumed >10 µg C d^{-1}. Larger organisms consumed substantially more, with 60-mm salps (large blastozooids) consuming 90 – 120 µg C d^{-1} during Cycles 1 and 2 and nearly 300 µg C d^{-1} during Cycle 4. 150-mm salps (large oozooids) consumed 300 – 400 µg C d^{-1} during Cycles 1 and 2 and nearly 1,000 µg C d^{-1} during Cycle 4. These estimates are likely underestimates of total ingestion, since they include only eukaryotic phytoplankton biomass. Aplastidic protists, cyanobacteria, and heterotrophic bacteria were also abundant and likely to be important prey items of *S. thompsoni*.

Discussion

Salp grazing rates, daily ration, and size selectivity – Our results show strong size dependence of clearance rates for *S. thompsoni* spanning a range of sizes and including both oozooids and blastozooids. Absolute clearance rates for the largest oozooids were >2 orders of magnitude higher than clearance rates for the smallest, newly-released blastozooids (Fig. 5). However, since the exponent of the power-law relationship relating salp total length to filtration rate (2.1 ± 0.02) was lower than the exponent relating salp volume to length (2.45, Iguchi and Ikeda 2004), salp volume-specific clearance rates were inversely related to length, decreasing from ~12,000 d^{-1} for newly released blasozooids to ~4,500 d^{-1} for large oozooids. Similarly, Madin et al. (2006) and Pakhomov et al. (2006) found that clearance rate normalized to organism biovolume decreased slightly with increasing size for *S. aspera* and *S. thompsoni*, respectively.

Combining Eq. 5 with phytoplankton size spectra data, we found that carbon-based ingestion rates increased from 4 – 12 µg C d^{-1} for a typical newly-released (6-mm) blastozooid to 300 – 1,000 µg C d^{-1} for a 150-mm oozooid. Using results from Iguchi and Ikeda (2004) to estimate carbon mass from total length, we estimate that a 6-mm blastozooid had a carbon mass of 31 µg C, suggesting that these salps were consuming an equivalent of between 13% and 39% of their carbon mass each day. For comparison, using both cohort-based growth analysis across wide size ranges and in situ experiments within a plankton kreisel, Lüskow et al. (2020) estimated length-based growth rates for *S. thompsoni* at the Chatham Rise of ~10% d^{-1}, which equates to a carbon-based growth rate of ~26% d^{-1}. Based on these calculations, a typical newly-released blastozooid would consume barely enough phytoplankton carbon to meet its growth needs (neglecting carbon lost to respiration or defecation). However, *S. thompsoni* is likely to consume many other prey items. Heterotrophic bacteria biomass ranged from 5.9 to 37 µg C L^{-1} in the mixed layer. Heterotrophic protists often have a biomass in the range of half of the phytoplankton biomass in the open ocean. *S. thompsoni* has also been shown to feed on a diverse suite of organisms larger than the 30-µm size cutoff that we used for phytoplankton, including eggs, nauplii and adult crustaceans, foraminifera, radiolarians, phaeodarians, pteropods, and non-living detritus including fecal pellets (Gowing 1989; Lancraft et al. 1991; von Harbou et al. 2011). Given these additional likely prey types, our grazing results seem remarkably consistent with simultaneous, but independent, measurements of growth rates.

Other studies have found variable ingestion rates for *S. thompsoni*. Von Harbou et al. (2011) found that daily ingestion could exceed body weight in the summer in the Lazarev Sea (although at substantially higher surface Chl *a* than at our study site), but was only 7 – 10% of body weight in the winter. Froneman et al. (1996) found daily rations of 73% d^{-1} in the ice-edge region of the Lazarev Sea. Huntley et al. (1989) estimated filtration rates of 4.1 – 9 L $salp^{-1}$ d^{-1} for 40-mm salps near the Antarctic Peninsula, compared to our estimate of 13 L $salp^{-1}$ d^{-1} (at warmer temperatures). Multiple studies have even estimated >100% of primary productivity consumed per day by salp communities (Dubischar and Bathmann 1997; Perissinotto et al. 1997; Bernard et al. 2012). However, these estimates have largely been based on only one or two net tows, rather than the extended sampling conducted during our Lagrangian experiments. Across the 23 bongo tows that we conducted during Cycle 1 (our longest Lagrangian study), calculated clearance rates on >10-µm phytoplankton ranged from 1% of biomass consumed d^{-1} for the tow with the lowest salp biomass to 30% d^{-1} for the tow with the highest salp biomass. This tow-to-tow variability (driven by the inherent patchiness of salp populations) can thus lead to substantial over- or under-estimation of average salp biomass and grazing pressure in a region if assessed from only a single tow. It is thus not surprising that our results (based on averaging 13 – 23 tows per cycle) fall near the mean range of prior estimates of salp grazing pressure.

One of the most important adaptations of pelagic tunicates is their fine feeding meshes that allow them to feed on organisms orders of magnitude smaller than themselves. Sutherland et al. (2010) has even suggested that *Pegea confoederata* can satisfy its energetic requirements through ingestion of <1.4-µm particles. Few studies, however, have directly quantified salp size-specific clearance rates on natural prey. Kremer and Madin (1992) found that *Pegea bicaudata* retention efficiencies were high for >2.5-µm beads, but substantially lower for smaller beads, with the exception of the smallest (15-mm) blastozooids assessed, which could feed efficiently on 1-µm beads. For other species assessed (*P. confoederata*, *Salpa aspera*, *Cyclosalpa polae* and *Brooksia rostrata*), the authors found uniformly low retention efficiencies for 1-µm beads regardless of salp length. Sutherland et al. (2010) found only slightly lower filtration rates for *P. confoederata* on 0.5- and 1-µm beads than on 3-µm beads. Harbison and Gilmer (1976) found that *P. confoederata* could feed on <1-µm cultured cyanobacteria (*Coccochloris* sp.). Caron et al. (1989) found negligible filtration rates on *Synechococcus* (<1 µm), moderate filtration rates on *Bodo* sp.(2 – 2.5 µm) and high filtration rates on *Isochrysis galbana* (5 µm) for *Cyclosalpa affinis*, *Salpa maxima*, and *P. confoederata*. Nishikawa et al. (2001) quantified size-fractionated chlorophyll concentrations in salp grazing incubation experiments and concluded that salp grazing rates were highest on 2 – 20-µm prey. Dadon-Pilosof et al. (2019) found substantially higher *S. maxima, Salpa fusiformis,* and *Thalia democratica* grazing rates on picoeukaryotes and nanoeukaryotes than on *Synechococcus, Prochlorococcus,* and heterotrophic bacteria. *Synechococcus* has also been found in the fecal pellets of salps (Pfannkuche and Lochte 1993), although this does not necessarily imply efficient feeding on cyanobacteria-sized cells, because mesozooplankton can also consume *Synechococcus* contained in aggregates (Stukel et al. 2013).

Our results are largely in line with these previous studies and show that *S. thompsoni* retention efficiency is lower when feeding on picoplankton than when feeding on nano- and microplankton. Our results do, however, show a distinct change in size selectivity with increasing size. The smallest blastozooids were able to feed efficiently on ~1-µm cells and had reasonably high clearance rates even for 0.4-µm cells. This gave them access to abundant picoplanktonic cells. Larger taxa (e.g., common 60-mm blastozooids or 100-mm oozooids), however, were only able to feed efficiently on nano- and micro-plankton cells. Despite differences in equivalent mesh diameter, our results suggest that the diets of differently sized salps was similar. Extensive flow cytometric analyses of samples from throughout the euphotic zone on each cycle (Fig. 3) showed that phytoplankton biomass was concentrated in the nano- and microphytoplankton size classes. All size classes of *S. thompsoni* thus derived the majority of their (phytoplankton) carbon from >8-µm phytoplankton (which still yields a predator:prey length ratio of >10,000:1 for the largest oozooids). Small blastozooids, however, would have had much greater access to the biomass (5.9 to 37 µg C L^{-1}) contained in heterotrophic bacteria in the mixed layer. For comparison, mean mixed layer eukaryotic phytoplankton biomass was 62, 88, and 101 µg C L^{-1}, for Cycles 1, 2, and 4, respectively. Prokaryotes were thus likely to be an important source of nutrition for newly-released blastozooids, although even for these small salps, the most important prey item was nano- and microphytoplankton.

Salp competitive interactions – In the Southern Ocean, *S. thompsoni* has often been considered a competitor of *E. superba*. The assumption of competitive interactions between these taxa stems, in part, from the fact that they are often the two dominant macrozooplankton species in the Southern Ocean, yet are commonly found in distinctly different water parcels (Pakhomov et al. 2002). Although some have hypothesized direct interactions between *E. superba* and *S. thompsoni* at various ontogenetic stages (Huntley et al. 1989), exploitation competition is most frequently invoked as the primary mode of interaction between the species; that is, salp grazing pressure exhausts the prey field necessary for successful *E. superba* feeding and vice versa (Loeb et al. 1997). However, the two species may fill distinctly different niches. *E. superba* thrives in diatom-dominated regions (Haberman et al. 2003), and may supplement its diet via substantial carnivory on

copepods and other taxa when microplankton are not abundant (Nordhausen et al. 1992; Cripps and Atkinson 2000). In contrast, *S. thompsoni* can feed on small phytoplankton and often excels in mesotrophic conditions (Zeldis et al. 1995; Pakhomov and Hunt 2017; Kelly et al. 2020). Indeed, our study shows that small *S. thompsoni* blastozooids can feed efficiently on cells as small as 1.2 µm, while even large (125-mm) oozooids could feed efficiently on cells >4.7 µm. Both groups derived over half of their (phytoplankton-based) nutrition from <10-µm cells that are largely unavailable to *E. superba* (although we note that *S. thompsoni* was likely deriving some nutrition from cells greater than our 30-µm cutoff, as well as cyanobacterial cells not assessed in this study). Blastozooids and oozoids also had the potential to derive substantial nutrition from even smaller cells if the phytoplankton community was dominated by picoplankton. These results suggest that salps and krill may not be direct competitors in the Southern Ocean. Rather, each flourishes in distinctly different conditions; krill during diatom blooms and salps in mesotrophic regions. Multiple studies have found that *S. thompsoni* abundances are often higher when Chl *a* concentrations are low (Pakhomov and Hunt 2017; Kelly et al. 2020). One explanation for the absence of *S. thompsoni* aggregations in diatom-dominated coastal regions is the potential for clogging of their feeding webs when plankton biomass is high (Harbison et al. 1986). Alternately, it is possible that *S. thompsoni* is hindered by low reproductive success in very cold waters (Henschke and Pakhomov 2018) or that the short (<1 y) life span of *S. thompsoni* makes it poorly adapted to highly seasonal waters along the Antarctic continent where prey concentrations may be too low to sustain growth, and indeed substantially reduced feeding has been measured in winter in the Lazarev Sea (von Harbou et al. 2011).

Regardless, it appears that even when they are abundant, as in this study, salps seldom exert higher grazing pressure than protists and hence are unlikely to prevent *E. superba* growth through competitive exclusion. Indeed, although protistan communities typically exert greater grazing pressure on picophytoplankton than on diatoms, diatom mortality due to protistan grazing is substantial in many regions (Selph et al. 2001; Sherr and Sherr 2007; Selph et al. 2011) and protistan grazing pressure often has no clear dependence on phytoplankton size (Taniguchi et al. 2014). Furthermore, in this study we found no significant decline in protistan grazing on large (30-µm) phytoplankton relative to picophytoplankton, suggesting that protists (rather than *S. thompsoni*) may prevent microplankton blooms that would benefit *E. superba*. Conversely, *E. superba* does not feed efficiently on the nanoplankton that were the most important salp prey in our study, and hence are unlikely to exclude *S. thompsoni*. Instead, it is protistan grazers that typically control pico- and nanophytoplankton biomass globally and in the Southern Ocean (Calbet and Landry 2004; Pearce et al. 2011; Latasa et al. 2014).

It thus may be more useful to assess competitive interactions between salps and protistan grazers. These organisms compete for similar prey items and both have life spans that can be similar to or shorter than the time scale of a Southern Ocean phytoplankton bloom. This allows both groups to respond reproductively to phytoplankton blooms. In fact, the ability of protists and salps to respond to increasing phytoplankton production may determine whether or not a bloom becomes too dense and causes salp mesh clogging (Harbison et al. 1986). Conversely, intense protistan grazing pressure has the potential to maintain phytoplankton biomass levels at concentrations too low for salps to consume sufficient carbon to satisfy their metabolic and growth requirements. It seems that in our study region, salp grazing rates (including consumption of heterotrophs and non-living material) were likely high enough to slightly exceed their daily requirements. More effective protistan grazing control, however, could potentially lead to reduced phytoplankton standing stock and insufficient ingestion rates to support salp growth. Indeed, Cycle 5 (the "non-salp" cycle with lowest salp biomass) had lower Chl *a* than the other cycles. We thus consider it likely that competition with protistan grazers may be an important ecological interaction for *S. thompsoni*.

Additionally, with their non-selective grazing abilities, salps have the potential to exert important grazing pressure on protistan competitors. This is particularly interesting given the difference in grazing threshold between mature oozooids (i.e., feeding efficiently only on >5-µm cells) and the chains of small blastozooids that they release (which fed effectively on picoplankton in our study). It is possible that direct consumption of nano- and microzooplankton by mature oozooids relieves grazing pressure on picoplankton, thus stimulating net growth of a potential prey item for their offspring. In support of this hypothesis, Cycle 1 (our cycle with the highest abundance of large oozooids) also had the highest relative contribution of picoeukaryotic phytoplankton (Fig. 3). Although we did not detect reduced protistan grazing pressure on picophytoplankton during this cycle (Fig. 4), this may have been due to our occupation of the water parcel soon after the release of substantial numbers of young blastozooids (Fig. 2), whose grazing activity may have already impacted the protistan community before our arrival.

Given these expected interactions between protists and *S. thompsoni*, it is worth considering expected shifts that would occur in pelagic ecosystems if a protist-dominated grazer community shifted to a mixed protist-salp community. One of the most important ecological differences between salps and protists is vastly different predatory:prey size ratios. Protistan zooplankton typically feed with a predator:prey size ratio (linear dimension) of between 3:1 and 5:1 with some dinoflagellates exhibiting a lower ratio of 1:1 and ciliates feeding at a 10:1 or higher size ratio (Sherr and Sherr 2007; Fuchs and Franks 2010; Dolan et al. 2013). In contrast, as shown here, *S. thompsoni* feeds at closer to a 10,000:1 predator:prey size ratio. This has profound implications for energy and matter transfer through food webs. Because of their high predator:prey size ratios, salps can efficiently shunt the productivity of pico- and nanophytoplankton carbon to larger nektonic predators (Henschke et al. 2016). Contrary to the prior assumption that salps (in contrast to euphausiids) were "trophic dead ends", when compared to protist-dominated communities, salp blooms should substantially increase food availability to fish and other top predators, and indeed many of these higher tropic level species have been found to feed on them (Cardona et al. 2012; Henschke et al. 2016).

Salps also alter the biogeochemical functionality of pelagic ecosystems, relative to their protist competitors. Protist grazing enhances nutrient regeneration and dissolved organic matter production through the microbial loop (Steinberg and Landry 2017). Although some large protists can produce slowly-sinking "mini" fecal pellets, it is generally safe to assume that the majority of the carbon and nitrogen consumed by protists will be recycled within the euphotic zone, with approximately 30% converted into protist biomass (Straile 1997). Most of this secondary production, however, will wind up being consumed by other links in the protistan food web, leading to only inefficient transfer to larger organisms (Landry and Calbet 2004). Salps, in contrast, produce rapidly-sinking fecal pellets that can substantially increase particle flux out of the upper ocean (Madin 1982; Stone and Steinberg 2016). Their carcasses can also contribute substantially to export flux (Henschke et al. 2013; Smith et al. 2014). It thus seems likely that, while salp blooms may increase trophic efficiency and enhance transfer to top predators, they may also decrease the duration of phytoplankton blooms by reducing remineralization rates. This may increase the variability and patchiness in food supply in the pelagic ocean with unknown effects on other taxa.

Despite these hypotheses about pelagic food web modifications in response to salp blooms, we caution that few studies have directly assessed the interactions between salps and protistan zooplankton. Understanding how Southern Ocean ecosystems will respond to a predicted southward expansion of *S. thompsoni* (Atkinson et al. 2004) thus requires answering key questions: Can salps exert top-down control on protistan zooplankton communities? How do the size spectra of ambient prey fields, salp clearance rates, and protistan clearance rates vary in time and space? Do salp and protistan zooplankton abundances and/or grazing impact covary in time and space? Do specific protistan taxa exhibit species-specific interactions with salps or their common prey items? How many trophic steps separate herbivorous protistan zooplankton from crustaceans and/or salps? What proportion of salp diets come from heterotrophic and/or mixotrophic protists? What is the role of bacterivory by protists and salps in Southern Ocean food webs? Answering these questions will require coordinated studies by protistan and salp ecologists, but has the potential to transform our understanding of these diverse organisms and their changing ecosystem.

Conclusion

Our experimental design allowed us to quantify size-specific grazing rates for salps and protistan grazers during the evolution of a *S. thompsoni* bloom. Salp filtration rates and equivalent mesh size were size dependent: the smallest (6-mm) blastozooids had filtration rates of ~0.2 L d^{-1} and could efficiently feed on cells greater than ~1-µm diameter, while the largest (150-mm) oozooids filtered >200 L d^{-1} but could only efficiently retain cells greater than ~6-µm diameter. These filtration rates, combined with high abundances at the beginning of the salp bloom, allowed the *S. thompsoni* community to clear ~8% of nano- and microphytoplankton biomass d^{-1}. Protistan zooplankton, however, were the dominant consumers of these prey items; daily, they consumed approximately 50% of all eukaryotic phytoplankton size classes (0.7 – 30 µm). This shows that protists are important competitors of salps despite the fact that these protists typically feed at less than a 10:1 predator:prey size ratio, while our results show

that the salps were mostly feeding at a predator:prey size ratio between 1,000:1 and 40,000:1.

References

Atkinson, A., V. Siegel, E. Pakhomov, and P. Rothery. 2004. Long-term decline in krill stock and increase in salps within the Southern Ocean. Nature **432:** 100-103. doi:10.1038/nature02950

Bernard, K. S., D. K. Steinberg, and O. M. E. Schofield. 2012. Summertime grazing impact of the dominant macrozooplankton off the Western Antarctic Peninsula. Deep-Sea Res. I **62:** 111-122. doi:10.1016/j.dsr.2011.12.015

Bone, Q. 1998. The biology of pelagic tunicates.

Bradford, J. 1985. Distribution of zooplankton off Westland, New Zealand, June 1979 and February 1982. New Zealand J. Mar. Fresh. Res. **19:** 311-326.

Bruland, K. W., and M. W. Silver. 1981. Sinking rates of fecal pellets from gelatinous zooplankton (salps, pteropods, doliolids). Mar. Biol. **63:** 295-300.

Calbet, A. 2008. The trophic roles of microzooplankton in marine systems. ICES J. Mar. Sci. **65:** 325-331. doi:10.1093/icesjms/fsn013

Calbet, A., and M. R. Landry. 2004. Phytoplankton growth, microzooplankton grazing, and carbon cycling in marine systems. Limnol. Oceanogr. **49:** 51-57.

Cardona, L., I. Álvarez de Quevedo, A. Borrell, and A. Aguilar. 2012. Massive Consumption of Gelatinous Plankton by Mediterranean Apex Predators. PloS one **7:** e31329. doi:10.1371/journal.pone.0031329

Caron, D. A., P. D. Countway, A. C. Jones, D. Y. Kim, and A. Schnetzer. 2012. Marine Protistan Diversity. Annu. Rev. Mar. Sci. **4:** 467-493. doi:10.1146/annurev-marine-120709-142802

Caron, D. A., L. P. Madin, and J. J. Cole. 1989. Composition and degradation of salp fecal pellets: Implications for vertical flux in oceanic environments. J. Mar. Res. **47:** 829-850.

Chiswell, S. M., J. Bradford-Grieve, M. G. Hadfield, and S. C. Kennan. 2013. Climatology of surface chlorophyll a, autumn-winter and spring blooms in the southwest Pacific Ocean. J. Geophys. Res. Oceans **118:** 1003-1018. doi:10.1002/jgrc.20088

Cripps, G., and A. Atkinson. 2000. Fatty acid composition as an indicator of carnivory in Antarctic krill, *Euphausia superba*. Can. J. Fish. Aquat. Sci. **57:** 31-37.

Dadon-Pilosof, A., F. Lombard, A. Genin, K. R. Sutherland, and G. Yahel. 2019. Prey taxonomy rather than size determines salp diets. Limnol. Oceanogr.

Décima, M., M. R. Stukel, L. López-López, and M. R. Landry. 2019. The unique ecological role of pyrosomes in the Eastern Tropical Pacific. Limnol. Oceanogr. **64:** 728-743. doi:10.1002/lno.11071

Dolan, J. R., D. J. S. Montagnes, S. Agatha, D. W. Coats, and D. K. Stoecker. 2013. The Biology and Ecology of Tintinnid Ciliates. Wiley-Blackwell.

Dubischar, C. D., and U. V. Bathmann. 1997. Grazing impact of copepods and salps on phytoplankton in the Atlantic sector of the Southern Ocean. Deep-Sea Res. II **44:** 415-433.

Froneman, P., E. Pakhomov, R. Perissinotto, and C. McQuaid. 1996. Role of microplankton in the diet and daily ration of Antarctic zooplankton species during austral summer. Mar. Ecol. Prog. Ser. **143:** 15-23.

Fuchs, H. L., and P. J. S. Franks. 2010. Plankton community properties determined by nutrients and size-selective feeding. Mar. Ecol. Prog. Ser. **413:** 1-15.

Garzio, L. M., D. K. Steinberg, M. Erickson, and H. W. Ducklow. 2013. Microzooplankton grazing along the Western Antarctic Peninsula. Aquat. Microb. Ecol. **70:** 215-232. doi:10.3354/ame01655

Gowing, M. 1989. Abundance and feeding ecology of Antarctic phaeodarian radiolarians. Mar. Biol. **103:** 107-118.

Haberman, K. L., R. M. Ross, and L. B. Quetin. 2003. Diet of the Antarctic krill (*Euphausia superba* Dana): II. Selective grazing in mixed phytoplankton assemblages. J. Exp. Mar. Biol. Ecol. **283:** 97-113.

Hansen, P. J., P. K. Bjornsen, and B. W. Hansen. 1997. Zooplankton grazing and growth: Scaling within the 2-2,000-mu m body size range. Limnol. Oceanogr. **42:** 687-704.

Harbison, G. R., and R. W. Gilmer. 1976. The feeding rates of the pelagic tunicate *Pegea confederata* and two other salps. Limnol. Oceanogr. **21:** 517-528.

Harbison, G. R., V. L. McAlister, and R. W. Gilmer. 1986. The response of the salp, *Pegea confoederata*, to high levels of particulate material: Starvation in the midst of plenty. Limnol. Oceanogr. **31:** 371-382.

Henschke, N. and others 2013. Salp-falls in the Tasman Sea: a major food input to deep-sea benthos. Mar. Ecol. Prog. Ser. **491:** 165-175.

Henschke, N., J. D. Everett, A. J. Richardson, and I. M. Suthers. 2016. Rethinking the Role of Salps in the Ocean. Trends Ecol. Evol. **31:** 720-733.

Henschke, N., and E. A. Pakhomov. 2018. Latitudinal variations in *Salpa thompsoni* reproductive fitness. Limnol. Oceanogr.

Huntley, M. E., P. F. Sykes, and V. Marin. 1989. Biometry and trophodynamics of Salpa thompsoni Foxton (Tunicata: Thaliacea) near the Antarctic Peninsula in austral summer, 1983–1984. Polar Biol. **10:** 59-70.

Iguchi, N., and T. Ikeda. 2004. Metabolism and elemental composition of aggregate and solitary forms of *Salpa thompsoni* (Tunicata: Thaliacea) in waters off the Antarctic Peninsula during austral summer 1999. J. Plankton Res. **26:** 1025-1037.

Kelly, P. and others 2020. Salpa thompsoni in the Indian Sector of the Southern Ocean: Environmental drivers and life history parameters. Deep-Sea Res. II**:** 104789.

Kremer, P., and L. P. Madin. 1992. Particle retention efficiency of salps. J. Plankton Res. **14:** 1009-1015. doi:10.1093/plankt/14.7.1009

Lancraft, T. M., T. L. Hopkins, J. J. Torres, and J. Donnelly. 1991. Oceanic micronektonic/macrozooplanktonic community structure and feeding in ice covered Antarctic waters during the winter (AMERIEZ 1988). Polar Biol. **11:** 157-167.

Landry, M. R., and A. Calbet. 2004. Microzooplankton production in the oceans. ICES J. Mar. Sci. **61:** 501-507.

Landry, M. R., L. W. Haas, and V. L. Fagerness. 1984. Dynamics of microbial plankton communities: experiments in Kaneohe Bay, Hawaii. Mar. Ecol. Prog. Ser. **16:** 127-133.

Landry, M. R., M. D. Ohman, R. Goericke, M. R. Stukel, and K. Tsyrklevich. 2009. Lagrangian studies of phytoplankton growth and grazing relationships in a coastal upwelling ecosystem off Southern California. Prog. Oceanogr. **83:** 208-216. doi:10.1016/j.pocean.2009.07.026

Landry, M. R., M. R. Stukel, and M. Décima. 2020. Food-web fluxes support high rates of mesozooplankton respiration and production in the equatorial Pacific. Mar. Ecol. Prog. Ser. **652:** 15-32.

Latasa, M., J. Henjes, R. Scharek, P. Assmy, R. Rottgers, and V. Smetacek. 2014. Progressive decoupling between phytoplankton growth and microzooplankton grazing during an iron-induced phytoplankton bloom in the Southern Ocean (EIFEX). Mar. Ecol. Prog. Ser. **513:** 39-50. doi:10.3354/meps10937

Loeb, V., V. Siegel, O. Holm-Hansen, and R. Hewitt. 1997. Effects of sea-ice extent and krill or salp dominance on the Antarctic food web. Nature **387:** 897.

Lüskow, F., E. A. Pakhomov, M. R. Stukel, and M. Décima. 2020. Biology of *Salpa thompsoni* at the Chatham Rise, New Zealand: demography, growth, and diel vertical migration. Mar. Biol. **167:** 175.

Madin, L., and C. Cetta. 1984. The use of gut fluorescence to estimate grazing by oceanic salps. J. Plankton Res. **6:** 475-492.

Madin, L., P. Kremer, P. Wiebe, J. Purcell, E. Horgan, and D. Nemazie. 2006. Periodic swarms of the salp *Salpa aspera* in the Slope Water off the NE United States: Biovolume, vertical migration, grazing, and vertical flux. Deep-Sea Res. I **53:** 804-819.

Madin, L. P. 1982. Production, composition, and sedimentation of salp fecal pellets in oceanic waters. Mar. Biol. **67:** 39-45.

Madin, L. P., and G. R. Harbison. 1977. The associations of Amphipod Hyperiidea with gelatinous zooplankton - I. Associations with Saplidae. Deep Sea Res. **24:** 449-463. doi:10.1016/0146-6291(77)90483-0

Madin, L. P., and J. E. Purcell. 1992. Feeding, metabolism, and growth of *Cyclosalpa bakeri* in the subarctic Pacific. Limnol. Oceanogr. **37:** 1236-1251.

Menden-Deuer, S., and E. J. Lessard. 2000. Carbon to volume relationships for dinoflagellates, diatoms, and other protist plankton. Limnol. Oceanogr. **45:** 569-579.

Nishikawa, J., and A. Tsuda. 2001. Feeding of the pelagic tunicate, *Salpa thompsoni*, on flagellates and size-fractionated chlorophyll particles. Plankton biology and ecology **48:** 133-135.

Nordhausen, W., M. Huntley, and M. D. G. Lopez. 1992. RACER: carnivory by *Euphausia superba* during the antarctic winter. Antarctic Journal of the United States **27:** 181-183.

Pakhomov, E. 2000. Demography and life cycle of Antarctic krill, *Euphausia superba*, in the Indian sector of the Southern Ocean: long-term comparison between coastal and open-ocean regions. Can. J. Fish. Aquat. Sci. **57:** 68-90.

Pakhomov, E., C. Dubischar, V. Strass, M. Brichta, and U. Bathmann. 2006. The tunicate *Salpa thompsoni* ecology in the Southern Ocean. I. Distribution, biomass, demography and feeding ecophysiology. Mar. Biol. **149:** 609-623.

Pakhomov, E. A., P. W. Froneman, and R. Perissinotto. 2002. Salp/krill interactions in the Southern Ocean: spatial segregation and implications for the carbon flux. Deep-Sea Res. II **49:** 1881-1907. doi:10.1016/S0967-0645(02)00017-6

Pakhomov, E. A., and B. P. Hunt. 2017. Trans-Atlantic variability in ecology of the pelagic tunicate *Salpa thompsoni* near the Antarctic Polar Front. Deep-Sea Res. II **138:** 126-140.

Pearce, I., A. T. Davidson, P. G. Thomson, S. Wright, and R. van den Enden. 2011. Marine microbial ecology in the sub-Antarctic Zone: Rates of bacterial and phytoplankton growth and grazing by heterotrophic protists. Deep-Sea Res. II **58:** 2248-2259. doi:10.1016/j.dsr2.2011.05.030

Perissinotto, R., E. Pakhomov, C. McQuaid, and P. Froneman. 1997. In situ grazing rates and daily ration of Antarctic krill *Euphausia superba* feeding on phytoplankton at the Antarctic Polar Front and the Marginal Ice Zone. Mar. Ecol. Prog. Ser. **160:** 77-91.

Pfannkuche, O., and K. Lochte. 1993. Open ocean pelago-benthic coupling: cyanobacteria as tracers of sedimenting salp feces. Deep-Sea Res. I **40:** 727-737.

Saba, G. K. and others 2014. Winter and spring controls on the summer food web of the coastal West Antarctic Peninsula. Nature Comm. **5**. doi:10.1038/ncomms5318

Selph, K. E., M. R. Landry, C. B. Allen, A. Calbet, S. Christensen, and R. R. Bidigare. 2001. Microbial community composition and growth dynamics in the Antarctic Polar Front and seasonal ice zone during late spring 1997. Deep-Sea Res. II **48:** 4059-4080. doi:10.1016/s0967-0645(01)00077-7

Selph, K. E. and others 2011. Spatially-resolved taxon-specific phytoplankton production and grazing dynamics in relation to iron distributions in the equatorial Pacific between 110 and 140°W. Deep-Sea Res. II **58:** 358-377. doi:10.1016/j.dsr2.2010.08.014

Sherr, E. B., and B. F. Sherr. 1994. Bacterivory and Herbivory - Key Roles of Phagotrophic Protists in Pelagic Food Webs. Microb. Ecol. **28:** 223-235.

---. 2007. Heterotrophic dinoflagellates: a significant component of microzooplankton biomass and major grazers of diatoms in the sea. Mar. Ecol. Prog. Ser. **352:** 187-197. doi:10.3354/meps07161

Smith, K. L., Jr. and others 2014. Large salp bloom export from the upper ocean and benthic community response in the abyssal northeast Pacific: Day to week resolution. Limnol. Oceanogr. **59:** 745-757. doi:10.4319/lo.2014.59.3.0745

Spiegelhalter, D. J., N. G. Best, B. P. Carlin, and A. Van Der Linde. 2002. Bayesian measures of model complexity and fit. Journal of the royal statistical society: Series b (statistical methodology) **64:** 583-639.

Steinberg, D. K., and M. R. Landry. 2017. Zooplankton and the ocean carbon cycle. Annu. Rev. Mar. Sci. **9:** 413-444.

Stone, J. P., and D. K. Steinberg. 2016. Salp contributions to vertical carbon flux in the Sargasso Sea. Deep-Sea Res. I **113:** 90-100. doi:10.1016/j.dsr.2016.04.007

Straile, D. 1997. Gross growth efficiencies of protozoan and metazoan zooplankton and their dependence on food concentration, predator-prey weight ratio, and taxonomic group. Limnol. Oceanogr. **42:** 1375-1385.

Strickland, J. D., and T. R. Parsons. 1972. A practical handbook of seawater analysis, second ed. Bull. Fish. Res. Board Can. **167**.

Stukel, M. R., M. Décima, K. E. Selph, D. A. A. Taniguchi, and M. R. Landry. 2013. The role of *Synechococcus* in vertical flux in the Costa Rica upwelling dome. Prog. Oceanogr. **112-113:** 49-59. doi:10.1016/j.pocean.2013.04.003

Sutherland, K. R., L. P. Madin, and R. Stocker. 2010. Filtration of submicrometer particles by pelagic tunicates. Proc. Natl. Acad. Sci. U. S. A. **107:** 15129-15134.

Sutton, P. 2001. Detailed structure of the subtropical front over Chatham Rise, east of New Zealand. J. Geophys. Res. Oceans **106:** 31045-31056.

Taniguchi, D. A. A., M. R. Landry, P. J. S. Franks, and K. E. Selph. 2014. Size-specific growth and grazing rates for picophytoplankton in coastal and oceanic regions of the eastern Pacific. Mar. Ecol. Prog. Ser. **509:** 87-101. doi:10.3354/meps10895

von Harbou, L., C. D. Dubischar, E. A. Pakhomov, B. P. Hunt, W. Hagen, and U. V. Bathmann. 2011. Salps in the Lazarev Sea, Southern Ocean: I. Feeding dynamics. Mar. Biol. **158:** 2009-2026.

Zeldis, J. R., C. S. Davis, M. R. James, S. L. Ballara, W. E. Booth, and F. H. Chang. 1995. Salp grazing: effects on phytoplankton abundance, vertical distribution and taxonomic composition in a coastal habitat. Mar. Ecol. Prog. Ser.**:** 267-283.

Zeldis, J. R., and M. Décima. 2020. Mesozooplankton connect the microbial food web to higher trophic levels and vertical export in the New Zealand Subtropical Convergence Zone. Deep-Sea Res. I **155:** 103146.

Acknowledgements

We would like to thank our many collaborators in the SalpPOOP project, especially Scott Nodder, Sadie Mills, Christian Fender, Florian Lüskow, Morgan Meyers, Sarah Searson, Siobhan O'Connor, Karl Safi, Adriana Lopes dos Santos, Fenella Deans, and Natalia Yingling. This research was funded by U.S. National Science Foundation awards #OCE-1756610 and 1756465 to M.R.S. and K.E.S., by the Ministry for Business, Innovation and Employment (MBIE) of New Zealand, by NIWA core programmes Coast and Oceans Food Webs (COES), Ocean Flows (COOF), and by the Royal Society of New Zealand Marsden Fast-track award to M.D. Data included in this study can be found on the Biological and Chemical Oceanography Data Management Office website (https://www.bco-dmo.org/project/754878).

Please cite as: Stukel, M. R., Decima, M., Selph, K. E., Gutierrez-Rodriguez, A. (2021). Size-specific grazing and competitive interactions between large salps and protistan grazers. Limnology and Oceanography. doi: 10.1002/lno.11770

Supplementary material for:

Size-specific grazing and competitive interactions between large salps and protistan grazers

Michael R. Stukel[1,2], Moira Décima[3,4], Karen Selph[5], Andres Gutiérrez-Rodríguez[3]

[1]Dept. of Earth, Ocean, and Atmospheric Science, Florida State University, Tallahassee, FL
[2]Center for Ocean-Atmospheric Prediction Studies, Florida State University, Tallahassee, FL
[3]National Institute of Water and Atmospheric Research (NIWA), Wellington, New Zealand
[4]Scripps Institution of Oceanography, University of California San Diego, SA
[5]Dept. of Oceanography, University of Hawaii at Manoa, Honolulu, HI
[*]Corresponding Author: mstukel@fsu.edu

ONLINE APPENDIX – SUPPLEMENTARY METHODS

Supp. Methods 1: Field Methods

Salp abundance and biomass estimation - Double oblique zooplankton net tows from 200 m water depth to the sea-surface were carried out using a 0.7 m-diameter Bongo frame with paired 200-µm mesh nets, equipped with two General Oceanics flow meters to measure the filtered volume and a temperature-depth recorder. Volume filtered per tow varied between 175 and 400 m^3. Tows were conducted at least twice daily (day and night), with one additional day per cycle of sampling every 2-3 h for further studies of diel patterns. Salps were sorted and identified to species using published keys (Thompson 1948; Foxton 1965; Bone 1998), staged into oozooid (solitary) or blastozooid (aggregate), measured for total length, and corrected to oral-to-atrial length (OAL) using conversions derived by Lüskow et al. (2020). A random subsample (10 specimens, when available) of each species/stage from each tow was taken for determination of Chl *a* in salp guts for grazing estimates. For further analyses, *S. thompsoni* total lengths were divided into 5-mm bins (5- to 140-mm) from which we computed normalized abundance size spectra (NASS = salp abundance within a bin divided by bin width). Biomass was calculated using length-frequency distributions (Iguchi and Ikeda 2004).

Protistan grazing experiments – We conducted daily two-point in situ protistan grazing dilution experiments in 2.25-L polycarbonate bottles at 6 depths in the water column (Landry et al. 1984; Landry et al. 2009). Initial samples were taken for flow cytometry and Chl *a* analyses from water gently transferred using silicon tubing to polycarbonate incubation bottles. A control bottle (100% whole seawater) and a "dilute" treatment bottle (25% whole seawater:75% 0.1-µm filtered seawater) were prepared directly from the same Niskin bottle at each depth. The whole seawater was not pre-screened to remove mesozooplankton, because the pre-screening process can kill delicate aloricate ciliates and disrupt chain-forming phytoplankton. All 12 bottles (6 depths × 2 bottles) were nutrient amended (9 µM $NaNO_3$, 1 µM NH_4Cl, 1 µM NaH_2PO_4, 11 µM $NaSiO_2$ (final concentrations) + vitamins and trace metals). A third, unamended whole seawater bottle at each depth was also prepared for growth rate determinations, although results are not used here. Bottles were then placed in mesh bags and incubated in situ on the drifting array for 24 h at the depths from which the samples were collected. After 24 h, the array was recovered, experimental bottles removed, and a new set of experimental bottles was attached to the array for deployment at the recovery location. After each 24 h recovery, final samples were taken for flow cytometry and Chl *a* analyses. Apparent growth rates in each bottle were calculated as $k = \ln(B_f/B_i)/\Delta t$, where B_f is the final phytoplankton carbon biomass, B_i is the initial phytoplankton biomass and Δt is the duration of the incubation (~1 d). Daily specific mortality rates due to protistan grazing were calculated as: $m = (k_{dil}-k_{whole})/(1\text{-dil})$, where k_{dil} is the growth rate in the diluted treatment bottle, k_{whole} is the growth rate in the control bottle, and dil is the fraction of whole seawater in the dilute treatment bottle (25%). Experiments were conducted for ~24 h.

Salp grazing experiments – To determine the size-specificity of salp grazing, we conducted grazing incubations on ship. At ~22:00 local time, paired 20-L plankton kreisels or 30-L pseudo-kreisels (circular or quasi-circular aquaria with radial flow, Raskoff et al. 2003) were gently filled (using silicon tubing) with mixed layer seawater collected by CTD-Niskin rosette casts. Salps for incubations were collected at ~23:00 local time using the salp net. The net was towed slowly and briefly (5 – 10 min) through the mixed layer. Healthy specimens, i.e., those that showed no physical damage, were then gently transferred (using a large ladle) into a bucket containing filtered surface seawater. Specimens were further observed (15 – 30 min) to ensure they actively swam (i.e., appeared healthy), then transferred into one of the paired kreisels, while the second kreisel was used as a control treatment (same mixed layer seawater; no salps). We successfully collected and incubated *S. thompsoni* blastozooids and oozooids ranging in size from 50 – 128 mm total length. We also conducted three incubations with a chain of blastozooids (6 – 8 mm individuals) released by an oozooid inside of one of the plankton kreisels. We found that this was the only way to successfully obtain such small blastozooids in healthy conditions. We also incubated a 112-mm *Thetys vagina* oozooid, although it did not feed on any of the phytoplankton size classes.

Water was circulated within the kreisels using a peristaltic pump and silicon tubing. Just after salp transfer to the kreisels, initial samples for flow cytometry were taken from each experimental and control kreisel. Additional time points were taken approximately every 2 h and analyzed in near real time to allow us to monitor salp grazing. Incubations typically lasted ~24 h. Of the 12 *S. thompsoni* incubations, one was terminated after only 4 h, because the organism was clearly unhealthy. Another incubation was run for 22 h without grazing detected on any size class of organism. These incubations were excluded from all subsequent calculations. In one experiment, after 15 h the abundance of protists suddenly increased by ~3-fold in samples taken from both the control and salp treatment kreisels. We assume that this was due to contamination in the sampling bottles and hence ignored all subsequent time points.

Gut pigment measurements – Because previous studies have shown that salp filtration rates can be underestimated when salps are incubated in a tank (Pakhomov et al. 2002), we also collected organisms for gut pigment analysis from bongo tows conducted multiple times daily (Madin and Cetta 1984). Organisms in one cod end were immediately anesthetized with soda water and salps were sized (OAL) and frozen (-80°C). They were later thawed, the guts excised and placed in 7-mL 90% acetone to extract (-4°C for 24 h). Chl *a* and phaeopigment content (together GPig, units = µg Chl *a* equivalents $salp^{-1}$) were then measured on a 10AU Turner fluorometer using the acidification method (Strickland and Parsons 1972; Décima et al. 2019). We estimated gut pigment turnover (GPT) time using the following equation GPT(h) = 2.607×ln(OAL, mm) - 2.6 , which was modified slightly from von Harbou et al. (2011) to include values from 4 gut clearance experiments conducted on SalpPOOP, that also supported the use of this equation for our water types. Chlorophyll-based grazing was estimated as: G (µg Chl *a* equiv. $salp^{-1}$ h^{-1}) = Gpig×GPT^{-1}.

Flow cytometry – Samples from the water column, protistan grazing dilution experiments, and salp incubations were analyzed at sea on a Becton-Dickinson Accuri C6 Plus flow cytometer to estimate the abundance and size of eukaryotic phytoplankton. Samples (660 µL) were run live within ~1-2 h of collection, discriminating on the Chl *a* fluorescence signal.

We estimated cell diameter from forward light scatter after developing a relationship based on analyses of multiple polystyrene bead sizes (0.99-10 µm diameter). We determined eukaryotic prey biomass from cell volume (assuming cells were spheres) using equations from Menden-Deuer and Lessard (2000). We note that forward scatter is an imperfect proxy for equivalent spherical diameter, and thus the absolute cell sizes determined in our study should be assumed to have associated uncertainty. Nevertheless, the net growth rates determined from this approach should be reliable, because all time points were analyzed using the same flow cytometer settings and rate determinations rely on differences as opposed to absolute magnitudes. Thus, grazing rates should be

unaffected by inaccuracies in cell size determination, although it is possible that cells we interpret as having a particular equivalent spherical diameter may actually have been slightly larger or smaller than that size.

Because the seagoing flow cytometer was not optimized for non-pigmented cells, we also preserved 2-mL samples with paraformaldehyde (0.5% final concentration), frozen at -80°C for shore-based analyses on a Beckman-Coulter CytoFLEX S flow cytometer. Batches of samples were stained for DNA with Hoechst 34580, and analyzed. Because preservation can cause cell shrinkage, we did not use forward scatter to analyze cell size for these preserved samples. Instead, we assumed that heterotrophic bacteria had a diameter of 0.4-µm and a carbon biomass of 11 fg C cell^{-1} (Garrison et al. 2000).

Size-specific grazing rate calculations – From each flow cytometry sample in the salp and protistan grazing rate experiments, we computed overlapping normalized biomass size spectra (NBSS) for eukaryotic phytoplankton. We used 17 evenly spaced logarithmic intervals with equivalent spherical diameters (ESD) ranging from 0.8 - 31 µm. Each bin extended from one half of the mid-point cell diameter to twice the mid-point cell diameter. Within each interval, we calculated the normalized biomass as:

$$B_n(ESD) = \sum_{\frac{ESD}{2}}^{2\times ESD} Biomass/(2 \times ESD - ESD/2)$$

Eq. 1

Net specific growth rates (k) of eukaryotic phytoplankton as a function of size in protistan grazing experiments were computed as $k(ESD) = \ln(B_{n,final}(ESD)/B_{n,initial}(ESD))/\Delta t$. Phytoplankton mortality due to protistan

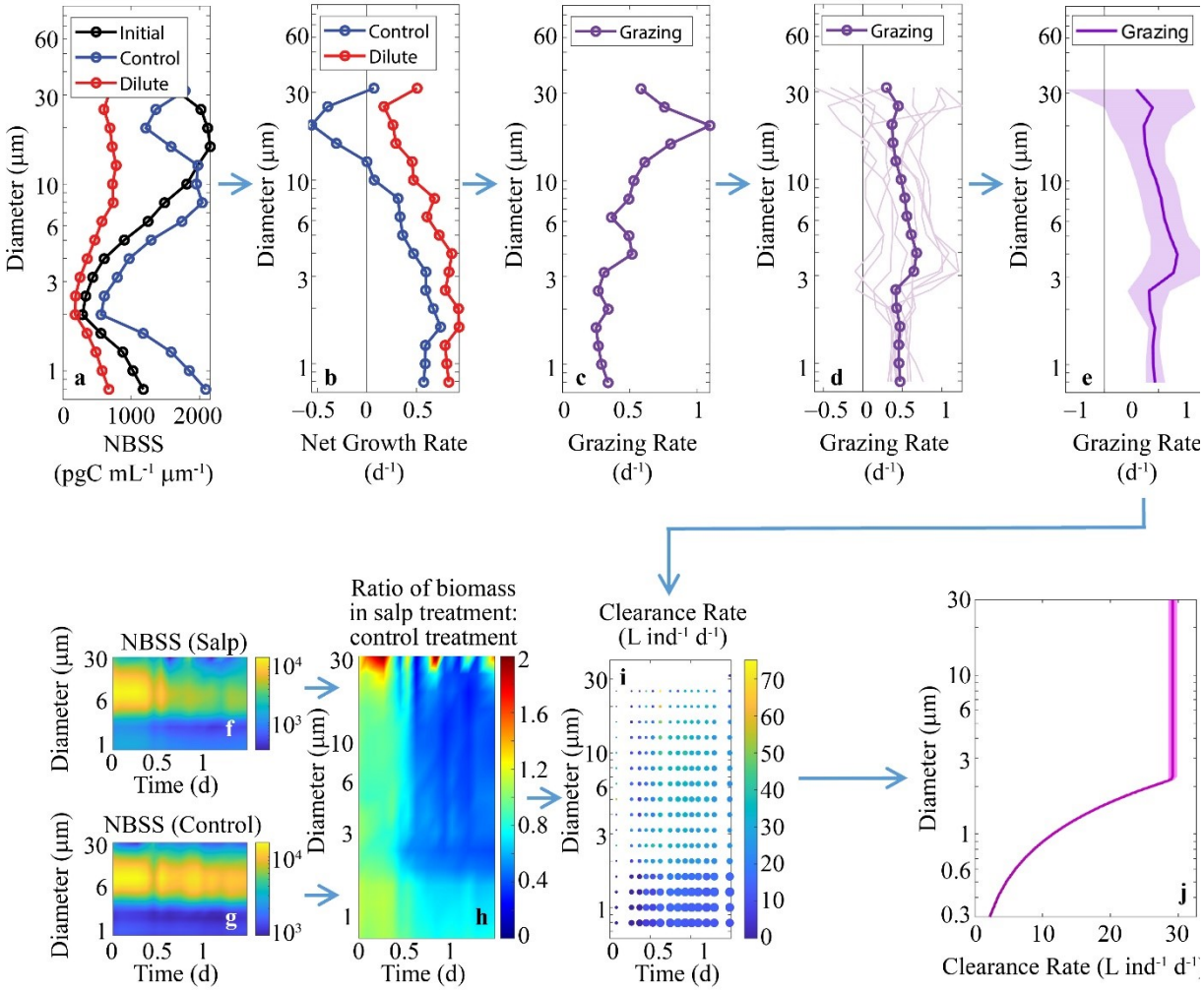

Supplementary Figure 1 – Overview of approach for quantifying size-specific salp clearance rates. We conducted daily protistan grazing dilution measurements at multiple depths in the mixed layer and quantified the normalized biomass size spectrum (NBSS) as a function of cell diameter from flow cytometry (FCM) initial and final samples of control and dilute experimental bottles (a). We then computed daily size-specific phytoplankton net growth rates in the dilute treatment (25% whole seawater:75% filtered seawater) and control (100% whole seawater) bottles (b), then size-specific phytoplankton mortality due to protistan grazing (c). Many grazing experiments were conducted for each Lagrangian cycle (d) and we used non-parametric bootstrapping to determine confidence limits on mean protistan grazing for the experimental cycle (e). In each salp grazing incubation, we took FCM samples ~every 2 h from the salp treatment kreisel (f) and the control (no salp) treatment kreisel (g) and computed NBSS. For each time point, we calculated the ratio of phytoplankton biomass in the salp treatment to that of the control treatment as a function of phytoplankton size (h). Using Eq. 2, for each time point we combined protistan grazing rates with the ratio of biomass in the salp to the control treatment to estimate clearance rate in each size bin (i). The dot size is inversely proportional to uncertainty from non-parametric Monte Carlo methods used to propagate uncertainty in biomass ratio and protistan grazing. We then used Bayesian approaches to determine salp clearance rates as a function of prey size (j).

grazing as a function of size (units of d^{-1}) were computed as m(ESD) = (k_{dil}(ESD) – k_{whole}(ESD))/(1-dil), where k_{dil} is the net growth rate in the dilute treatment, k_{whole} is the net growth rate in the whole seawater (control) treatment, and dil is the dilution ratio (25%). To determine an average grazing rate for each Lagrangian cycle, we averaged all grazing rate estimates, m(ESD), made in the mixed layer during that cycle (Supp. Fig. 1).

If we assume that grazing rates are constant throughout a 24-h period (a reasonable assumption in our experiments which were maintained at constant conditions in the dark) and that the dominant protistan grazers are in a size range that is efficiently retained by feeding salps, we can compute protistan grazing rate-corrected size-specific mortality of phytoplankton within an incubation due to salp grazing (G, units of d^{-1}) as:

$$G(ESD) = \frac{m(ESD)\left(\left(\frac{vol}{f_i N}\right)\left(e^{-\frac{f_i \times N}{vol}t}-1\right)+t\right)-\ln\left(\frac{B_{n,t}(ESD,t)}{B_{n,c}(ESD,t)}\right)}{t} \quad \text{Eq. 2}$$

where $B_{n,c}$ is the normalized biomass in the control kreisel at time t, $B_{n,t}$ is the normalized biomass in the treatment kreisel (with salps) at time t, vol is the volume of the kreisel, N is the number of salps in the treatment kreisel, and f_i is an initial estimate of salp filtration rate (determined from final/initial concentrations of nanophytoplankton in the incubation, units of L $salp^{-1}$ d^{-1}). G(ESD) relates to the actual clearance rate of the salps (C, units of L $salp^{-1}$ d^{-1}) through the equation: C(ESD)=G(ESD)/N/vol. We determined uncertainty in m(ESD) and G(ESD) through non-parametric bootstrapping techniques. For derivation of Eq. 2, see the online supplement.

Supp. Methods 2: Bayesian parameter estimation and model selection

For every incubation, we determined a smooth equation for clearance rate as a function of the ESD of the prey using two simple models. The first model assumes that clearance rates depend only on the filtration rate and filter mesh of the salp. It fits clearance rate using a two-parameter function in which F is the filtration rate of the salp and τ is a parameter that is approximately equal to the equivalent mesh size of the salp:

$$Clearance(ESD) = \min\left(\frac{\left(ESD/\tau\right)^2}{0.16+\left(ESD/\tau\right)^2}, 1\right) \times F \quad \text{Eq. 3}$$

The second equation is a three-parameter model that adds a functional form representing potential escape responses of prey, assuming that prey swimming velocity is proportional to size:

$$Clearance(ESD) = \min\left(\frac{\left(ESD/\tau\right)^2}{0.16+\left(ESD/\tau\right)^2}, 1\right) \times e^{-\lambda \cdot ESD} \times F \quad \text{Eq. 4}$$

where λ is a parameter that describes the evasion success of prey. Derivation of these equations is given in Supp. Methods 3. To fit these parameters to the incubation data, we used a Bayesian statistical framework solved with a Markov Chain Monto Carlo random walk and the Metropolis algorithm (Metropolis et al. 1953). We used weak uniform positive priors for F, τ, and λ. To avoid impacts associated with either delayed grazing as organisms adjusted to the kreisels or diel patterns in grazing, we removed all data points collected during the first 8 hours of each incubation. To objectively choose whether Eq. 3 or 4 was more appropriate for each incubation, we used deviance information criterion (DIC, Spiegelhalter et al. 2002). A model with a lower DIC is a better fit to the data.

To investigate how filtration rate and equivalent mesh size varied with salp body length, we also fit allometric-scaling relationships to the data from all of the incubations of the form:

$$Clearance(ESD) = \varphi \times TL^{\psi} \times \min\left(\frac{\left(ESD/\theta \times TL^{\gamma}\right)^2}{0.16+\left(ESD/\theta \times TL^{\gamma}\right)^2}, 1\right) \times Q_{10}^{(T-12°C)/10} \quad \text{Eq. 5}$$

$$Clearance(ESD) = \varphi \times TL^{\psi} \times \min\left(\frac{\left(ESD/\tau\right)^2}{0.16+\left(ESD/\tau\right)^2}, 1\right) \times Q_{10}^{(T-12°C)/10} \quad \text{Eq. 6}$$

Where TL is salp total length, $\varphi \times TL^{\psi}$ is an allometric-scaling relationship for the filtration rate, $\theta \times TL^{\gamma}$ is an allometric-scaling relationship for τ (the equivalent mesh diameter), T is temperature, and Q_{10} is a temperature scaling factor that we assume is equal to 2 (Madin and Purcell 1992). Eq. 6 assumes that τ does not vary with salp size. We again chose between the two equations based on DIC. In both of these equations we assume that avoidance is generally negligible, a conclusion that we reached based on the results from individual incubations (see Results).

We assume that this approach will give an accurate estimate of how size selectivity varies with prey length, because size selectivity is mostly determined by the mesh size of the salps, which should not vary between salps in the incubator and in situ. However, as noted above, salp filtration rates are often lower when incubated in shipboard tanks than when grazing in situ. Hence, we also fit Eq. 5 (which was found to be a better predictor than Eq. 6, see Results) to gut pigment data results. For this analysis, we combined in situ mixed layer carbon-based NBSS with mixed layer size-fractionated Chl *a* measurements (0.2-2, 2-20, >20-µm) to determine in situ Chl *a*-based NBSS (i.e., the concentration of Chl *a* contained within smoothly varying size fractions of phytoplankton). We then fit Eq. 5 to the results of Chl *a*-based consumption rates (mg Chl *a* h^{-1}) determined from gut pigment measurements.

Supp. Methods 3: Derivation of prostistan-grazing corrected salp clearance rates

In our control plankton kreisel (without salps), the rate of change of the biomass of cells with a specific equivalent spherical diameter (B_c(ESD)) will be equal to:

$$\frac{dB_c(ESD,t)}{dt} = \left(\mu(ESD) - m(ESD)\right) \times B_c(ESD,t) \quad \text{(A1)}$$

where µ(ESD) is the growth rate (d^{-1}) of cells of size ESD, and m(ESD) is the mortality rate (d^{-1}) of cells of size ESD due to protistan grazing. We assume that both µ(ESD) and m(ESD) are constant throughout the incubation. We also assume that m(ESD) is equal to the average mixed layer protistan grazing rate for the Lagrangian cycle from which the salps (and incubation water) were collected. However, we assume that the growth rate (which will depend on light and nutrients) in the incubation is not known. We can solve this differential equation and show that:

$$B_c(ESD,t) = B_0(ESD) \times e^{(\mu(ESD)-m(ESD)) \times t} \quad \text{(A2)}$$

where B_0(ESD) is the initial biomass in the incubation. We can write a similar equation for the rate of change of size-specific biomass in the treatment incubation (B_t(ESD)) as:

$$\frac{dB_t(ESD,t)}{dt} = \left(\mu(ESD) - m_*(ESD,t) - G(ESD)\right) \times B_t(ESD,t) \quad \text{(A3)}$$

Here, G(ESD) is the mortality (d^{-1}) experienced by phytoplankton in the incubation as a result of grazing by salps. Notably, G will relate to the clearance rate of salps (as a function of size) through the equation: C(ESD)=G(ESD)/N/vol, where C(ESD) is the clearance rate of salps, N is the number of salps in the incubation kreisel and vol is the volume of the incubation kreisel. m_*(ESD,t) is the mortality of phytoplankton due to protistan grazing. Unlike in eq. A1, m_*(ESD,t) in eq. A3 is a function of time, because salps remove protistan grazers from the incubation at the same time that they remove phytoplankton. We make the simplifying assumption that protistan grazers have a large enough size to be efficiently removed by salps. Hence we can calculate that:

$$m_*(ESD,t) = m(ESD) \times e^{-\frac{f_i N}{vol}t} \quad \text{(A4)}$$

where f_i is an initial estimate for the filtration rate of individual salps in the incubation (determined from salp clearance rates based on bulk nanophytoplankton without a correction for protistan grazing). Substituting Eq. A4 into Eq. A3 yields:

$$\frac{dB_t(ESD,t)}{dt} = \left(\mu(ESD) - m(ESD) \times e^{-\frac{f_i \times N}{vol}t} - G(ESD)\right) \times B_t(ESD,t) \quad \text{(A5)}$$

We can rearrange this equation to separate variables and then integrate to show that:

$$\ln(B_t(ESD,t)) = \left(\mu(ESD) - G(ESD)\right)t - m(ESD)\left(\frac{-vol}{f \times N}\right)e^{-\frac{f \times N}{vol}t} + Y \quad \text{(A6)}$$

Rearranging this equation, and setting $B_t(ESD,0) = B_0$ allows us to solve for Y and show that:

$$B_t(ESD,t) = B_0(ESD) \times e^{\mu(ESD)t} \times e^{m(ESD)\left(\frac{vol}{f \times N}\right)\left(e^{-\frac{f \times N}{vol}t}-1\right)} \times e^{-G(ESD)t} \quad \text{(A7)}$$

We have two unknowns in this equation (µ and G). To eliminate µ we can take the ratio of the biomass of phytoplankton in the treatment kreisel to the biomass of cells in the control kreisel:

$$\frac{B_t(ESD,t)}{B_c(ESD,t)} = \frac{B_0(ESD) \times e^{\mu(ESD) \times t} \times e^{m(ESD)\left(\frac{vol}{f \times N}\right)\left(e^{-\frac{f \times N}{vol}t}-1\right)} \times e^{-G(ESD) \times t}}{B_0(x) \times e^{(\mu(x)-m(x)) \times t}} \quad \text{(A8)}$$

We can then solve this equation with respect to G:

$$G(ESD) = \frac{m(ESD)\left(\left(\frac{vol}{f \times N}\right)\left(e^{-\frac{f \times N}{vol}t}-1\right)+t\right)-\ln\left(\frac{B_t(ESD,t)}{B_c(ESD,t)}\right)}{t} \quad \text{(A9)}$$

Please cite as: Stukel, M. R., Decima, M., Selph, K. E., Gutierrez-Rodriguez, A. (2021). Size-specific grazing and competitive interactions between large salps and protistan grazers. Limnology and Oceanography. doi: 10.1002/lno.11770

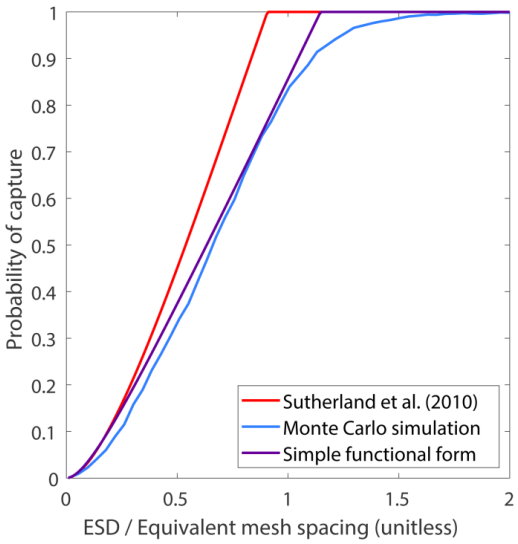

Supp. Fig. 2 – Probability that a prey cell will be captured. As the x-axis we use a unitless metric that is equal to prey equivalent spherical diameter divided by the equivalent mesh spacing as defined in Sutherland et al. (2010).

Supp. Methods 4: Derivation of simplified size-specific salp clearance rate functional form

Silvester (1983) and Sutherland et al. (2010) give mechanistic equations for the efficiency of salp filtration as a function of prey size from three measurable parameters: the diameter of individual fibers within salp filter meshes, the average width between fibers (narrow dimension) and the average length between fibers (long dimension). The functional form of this equation is shown in red in Supp. Fig 2. This equation, however, makes two important assumptions. It assumes that prey are spherical and that the mesh width is perfectly constant. If we relax these equations, we cannot find a closed-form solution to the equation, but we can estimate the functional form using a Monte Carlo approach where we simulate individual prey encounters in which the individual prey are given random widths (drawn from a uniform distribution) and random length:width ratios (drawn from the distribution shown in Supp. Fig. 3). We also randomly choose different length and widths for the salp mesh in the vicinity of the area where each prey cell encounters the salp. These lengths and widths are drawn from normal distributions in which the standard deviation is assumed to be 10% of the mean. We assume that each cell has the shape of a prolate sphere and that it is oriented in the flow such that its long axis is parallel to the flow. We then compute whether or not the cell will be captured by the salp based on the cell's width, the modified width and length of the salp mesh, and the equations in Silvester (1983) and Sutherland et al. (2010). The results are shown in the blue line in Supp. Fig. 2 and indicate that when variability in prey length:width and mesh spacing are included the theoretical efficiency of capture drops slightly. We introduce a simpler, one-parameter model that approximates these results:

$$\varepsilon(ESD,\tau) = \min\left(\frac{(ESD/\tau)^2}{0.16+(ESD/\tau)}, 1\right) \quad \text{(A10)}$$

Where τ is the equivalent mesh spacing of the salp and the value 0.16 represents the proportion of the area of a salp filtration mesh that is actually comprised of the fibers (rather than the gaps between fibers) and is estimated from values given in Sutherland et al. (2010). This equation is essentially equal to the mechanistic functional forms (to within the uncertainty limits with which flow cytometry can be used to diagnose prey diameter) and relies on only a single parameter (which should be approximately equal to the equivalent mesh spacing), providing more robust parameter estimation.

We also considered the possibility that capture efficiency could decrease with increasing prey size for larger prey, as a result of predator avoidance mechanisms. To simulate what the functional form of such behavior might look like, we assumed that prey swimming speed is proportional to prey diameter. We further assumed that all prey sense the flow disturbance created by salp filtration at the same distance from a salp, at which time they exhibit a simple avoidance behavior that consists of swimming in a random direction (in three dimensions) at their maximum swimming velocity. We assume that the prey are initially randomly distributed (in two-dimensions) within the flow stream created by the salp. If their escape maneuver allows them to reach a distance greater than the radius of the salp's oral aperture from the center of the flow before they reach the oral aperture, we assume they have escaped. We conducted a Monte Carlo simulation of such behavior (blue line in Supp. Fig. 4). As above, we chose to approximate this behavior using a simple one-parameter function:

$$\omega(ESD,\lambda) = e^{-\lambda \times ESD} \quad \text{(A11)}$$

Functionally, the parameter λ will depend on the assumed speed (body lengths per second) of prey, the distance at which prey sense the turbulence created by salp feeding, the velocity of the salp feeding current, and the radius of the salp's oral aperture. We then considered two models for salp clearance rate. The first assumes that prey evasion (Eq. A11) is insignificant and can be ignored, thus:

$$Clearance(ESD) = F \times \varepsilon(ESD,\tau) \quad \text{(A12)}$$

where F is the filtration rate of a salp. The second equation assumes that prey evasion is significant:

$$Clearance(ESD) = F \times \varepsilon(ESD,\tau) \times \omega(ESD,\lambda) \quad \text{(A13)}$$

We used a Bayesian model selection approach to fit the parameters F, λ, and τ for each salp grazing incubation and to determine (for each incubation) whether Eq. A12 or Eq. A13 were more appropriate.

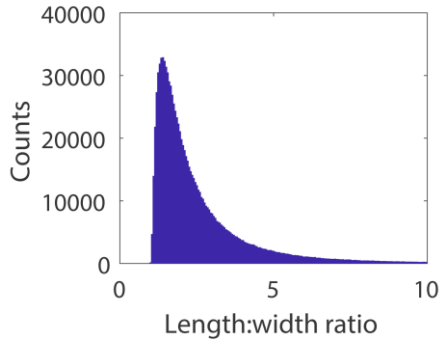

Supp. Fig. 3 – Length:width ratio distribution used in Monte Carlo simulation in Supp. Fig. 1.

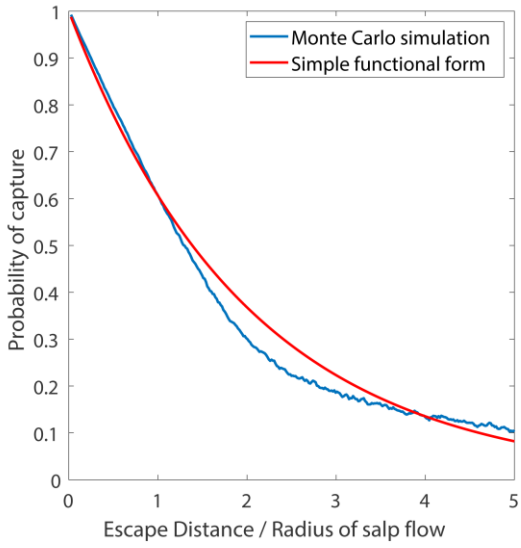

Supp. Fig. 4 – Decrease in filtration efficiency as a result of prey evasion behavior.

We also developed an allometric equation that can be used to estimate clearance rates for salps as a function of salp total length (TL) and prey size. In developing these equations, we started with Eq. A12 (because results showed that prey evasion was not substantial), but assumed that parameters F and τ have power law relationships with salp length. Thus we can write that:

$$F(TL) = \varphi \times TL^{\psi} \quad \text{(A14)}$$

$$\tau(TL) = \theta \times TL^{\gamma} \quad \text{(A15)}$$

Since each experiment took place at a slightly different temperature, we also assumed temperature-sensitivity of salp filtration rates with $Q_{10} = 2$. This yields an equation for clearance rate as a function of salp total length and prey diameter of:

$$Clearance(ESD) = \varphi \times TL^{\psi} \times \min\left(\frac{\left({ESD}/{(\theta \times TL^{\gamma})}\right)^2}{0.16+\left({ESD}/{(\theta \times TL^{\gamma})}\right)}, 1\right) \times Q_{10}{}^{(T-12°C)/10} \quad \text{(A16)}$$

We also considered a simpler model in which salp filtration rates (F), but not equivalent mesh diameter (τ), is a function of salp length:

$$Clearance(ESD) = \varphi \times TL^{\psi} \times \min\left(\frac{\left({ESD}/{\tau}\right)^2}{0.16+\left({ESD}/{\tau}\right)}, 1\right) \times Q_{10}{}^{(T-12°C)/10} \quad \text{(A17)}$$

We again used a Bayesian model selection approach to fit the parameters φ, ψ, θ, γ, and τ and decide whether Eq. A17 or Eq. A18 were more important. However, this time we fit the model to all incubation experiments simultaneously.

References

Atkinson, A., V. Siegel, E. Pakhomov, and P. Rothery. 2004. Long-term decline in krill stock and increase in salps within the Southern Ocean. Nature **432:** 100-103. doi: 10.1038/nature02950.

Bernard, K. S., D. K. Steinberg, and O. M. E. Schofield. 2012. Summertime grazing impact of the dominant macrozooplankton off the Western Antarctic Peninsula. Deep-Sea Res. I **62:** 111-122. doi: 10.1016/j.dsr.2011.12.015.

Bone, Q. 1998. The biology of pelagic tunicates.

Bradford, J. 1985. Distribution of zooplankton off Westland, New Zealand, June 1979 and February 1982. New Zealand Journal of Marine and Freshwater Research **19:** 311-326.

Bruland, K. W., and M. W. Silver. 1981. Sinking rates of fecal pellets from gelatinous zooplankton (salps, pteropods, doliolids). Mar. Biol. **63:** 295-300.

Calbet, A. 2008. The trophic roles of microzooplankton in marine systems. ICES J. Mar. Sci. **65:** 325-331. doi: 10.1093/icesjms/fsn013.

Calbet, A., and M. R. Landry. 2004. Phytoplankton growth, microzooplankton grazing, and carbon cycling in marine systems. Limnol. Oceanogr. **49:** 51-57.

Cardona, L., I. Álvarez de Quevedo, A. Borrell, and A. Aguilar. 2012. Massive Consumption of Gelatinous Plankton by Mediterranean Apex Predators. PloS one **7:** e31329. doi: 10.1371/journal.pone.0031329.

Caron, D. A., P. D. Countway, A. C. Jones, D. Y. Kim, and A. Schnetzer. 2012. Marine Protistan Diversity. Annu. Rev. Mar. Sci. **4:** 467-493. doi: 10.1146/annurev-marine-120709-142802.

Caron, D. A., L. P. Madin, and J. J. Cole. 1989. Composition and degradation of salp fecal pellets: Implications for vertical flux in oceanic environments. J. Mar. Res. **47:** 829-850.

Chiswell, S. M., J. Bradford-Grieve, M. G. Hadfield, and S. C. Kennan. 2013. Climatology of surface chlorophyll a, autumn-winter and spring blooms in the southwest Pacific Ocean. J. Geophys. Res. Oceans **118:** 1003-1018. doi: https://doi.org/10.1002/jgrc.20088.

Cripps, G., and A. Atkinson. 2000. Fatty acid composition as an indicator of carnivory in Antarctic krill, *Euphausia superba*. Canadian Journal of Fisheries and Aquatic Sciences **57:** 31-37.

Dadon-Pilosof, A., F. Lombard, A. Genin, K. R. Sutherland, and G. Yahel. 2019. Prey taxonomy rather than size determines salp diets. Limnol. Oceanogr.

Décima, M., M. R. Stukel, L. López-López, and M. R. Landry. 2019. The unique ecological role of pyrosomes in the Eastern Tropical Pacific. Limnol. Oceanogr. **64:** 728-743. doi: 10.1002/lno.11071.

Dolan, J. R., D. J. S. Montagnes, S. Agatha, D. W. Coats, and D. K. Stoecker. 2013. The Biology and Ecology of Tintinnid Ciliates. Wiley-Blackwell.

Dubischar, C. D., and U. V. Bathmann. 1997. Grazing impact of copepods and salps on phytoplankton in the Atlantic sector of the Southern Ocean. Deep-Sea Res. II **44:** 415-433.

Foxton, P. 1965. An aid to the detailed examination of salps [Tunicata: Salpidae]. Journal of the Marine Biological Association of the United Kingdom **45:** 679-681.

Froneman, P., E. Pakhomov, R. Perissinotto, and C. McQuaid. 1996. Role of microplankton in the diet and daily ration of Antarctic zooplankton species during austral summer. Mar. Ecol. Prog. Ser. **143:** 15-23.

Fuchs, H. L., and P. J. S. Franks. 2010. Plankton community properties determined by nutrients and size-selective feeding. Mar. Ecol. Prog. Ser. **413:** 1-15.

Garrison, D. L. and others 2000. Microbial food web structure in the Arabian Sea: a US JGOFS study. Deep-Sea Res. II **47:** 1387-1422.

Garzio, L. M., D. K. Steinberg, M. Erickson, and H. W. Ducklow. 2013. Microzooplankton grazing along the Western Antarctic Peninsula. Aquatic Microbial Ecology **70:** 215-232. doi: 10.3354/ame01655.

Gowing, M. 1989. Abundance and feeding ecology of Antarctic phaeodarian radiolarians. Mar. Biol. **103:** 107-118.

Haberman, K. L., R. M. Ross, and L. B. Quetin. 2003. Diet of the Antarctic krill (*Euphausia superba* Dana): II. Selective grazing in mixed phytoplankton assemblages. Journal of Experimental Marine Biology and Ecology **283:** 97-113.

Hansen, P. J., P. K. Bjornsen, and B. W. Hansen. 1997. Zooplankton grazing and growth: Scaling within the 2-2,000-mu m body size range. Limnol. Oceanogr. **42:** 687-704.

Harbison, G. R., and R. W. Gilmer. 1976. The feeding rates of the pelagic tunicate *Pegea confederata* and two other salps. Limnol. Oceanogr. **21:** 517-528.

Harbison, G. R., V. L. McAlister, and R. W. Gilmer. 1986. The response of the salp, *Pegea confoederata*, to high levels of particulate material: Starvation in the midst of plenty. Limnol. Oceanogr. **31:** 371-382.

Henschke, N. and others 2013. Salp-falls in the Tasman Sea: a major food input to deep-sea benthos. Mar. Ecol. Prog. Ser. **491:** 165-175.

Henschke, N., J. D. Everett, A. J. Richardson, and I. M. Suthers. 2016. Rethinking the Role of Salps in the Ocean. Trends in Ecology & Evolution **31:** 720-733.

Henschke, N., and E. A. Pakhomov. 2018. Latitudinal variations in *Salpa thompsoni* reproductive fitness. Limnol. Oceanogr.

Huntley, M. E., P. F. Sykes, and V. Marin. 1989. Biometry and trophodynamics of Salpa thompsoni Foxton (Tunicata: Thaliacea) near the Antarctic Peninsula in austral summer, 1983–1984. Polar Biol. **10:** 59-70.

Iguchi, N., and T. Ikeda. 2004. Metabolism and elemental composition of aggregate and solitary forms of *Salpa thompsoni* (Tunicata: Thaliacea) in waters off the Antarctic Peninsula during austral summer 1999. J. Plankton Res. **26:** 1025-1037.

Kelly, P. and others 2020. Salpa thompsoni in the Indian Sector of the Southern Ocean: Environmental drivers and life history parameters. Deep-Sea Res. II**:** 104789.

Kremer, P., and L. P. Madin. 1992. Particle retention efficiency of salps. J. Plankton Res. **14:** 1009-1015. doi: 10.1093/plankt/14.7.1009.

Lancraft, T. M., T. L. Hopkins, J. J. Torres, and J. Donnelly. 1991. Oceanic micronektonic/macrozooplanktonic community structure and feeding in ice covered Antarctic waters during the winter (AMERIEZ 1988). Polar Biol. **11:** 157-167.

Landry, M. R., and A. Calbet. 2004. Microzooplankton production in the oceans. ICES J. Mar. Sci. **61:** 501-507.

Landry, M. R., L. W. Haas, and V. L. Fagerness. 1984. Dynamics of microbial plankton communities: experiments in Kaneohe Bay, Hawaii. Mar. Ecol. Prog. Ser. **16:** 127-133.

Landry, M. R., M. D. Ohman, R. Goericke, M. R. Stukel, and K. Tsyrklevich. 2009. Lagrangian studies of phytoplankton growth and grazing relationships in a coastal upwelling ecosystem off Southern California. Prog. Oceanogr. **83:** 208-216. doi: 10.1016/j.pocean.2009.07.026.

Landry, M. R., M. R. Stukel, and M. Décima. 2020. Food-web fluxes support high rates of mesozooplankton respiration and production in the equatorial Pacific. Mar. Ecol. Prog. Ser. **652:** 15-32.

Latasa, M., J. Henjes, R. Scharek, P. Assmy, R. Rottgers, and V. Smetacek. 2014. Progressive decoupling between phytoplankton growth and

microzooplankton grazing during an iron-induced phytoplankton bloom in the Southern Ocean (EIFEX). Mar. Ecol. Prog. Ser. **513:** 39-50. doi: 10.3354/meps10937.

Loeb, V., V. Siegel, O. Holm-Hansen, and R. Hewitt. 1997. Effects of sea-ice extent and krill or salp dominance on the Antarctic food web. Nature **387:** 897.

Lüskow, F., E. A. Pakhomov, M. R. Stukel, and M. Décima. 2020. Biology of *Salpa thompsoni* at the Chatham Rise, New Zealand: demography, growth, and diel vertical migration. Mar. Biol. **167:** 175.

Madin, L., and C. Cetta. 1984. The use of gut fluorescence to estimate grazing by oceanic salps. J. Plankton Res. **6:** 475-492.

Madin, L., P. Kremer, P. Wiebe, J. Purcell, E. Horgan, and D. Nemazie. 2006. Periodic swarms of the salp *Salpa aspera* in the Slope Water off the NE United States: Biovolume, vertical migration, grazing, and vertical flux. Deep-Sea Res. I **53:** 804-819.

Madin, L. P. 1982. Production, composition, and sedimentation of salp fecal pellets in oceanic waters. Mar. Biol. **67:** 39-45.

Madin, L. P., and G. R. Harbison. 1977. The associations of Amphipod Hyperiidea with gelatinous zooplankton - I. Associations with Saplidae. Deep Sea Res. **24:** 449-463. doi: 10.1016/0146-6291(77)90483-0.

Madin, L. P., and J. E. Purcell. 1992. Feeding, metabolism, and growth of *Cyclosalpa bakeri* in the subarctic Pacific. Limnol. Oceanogr. **37:** 1236-1251.

Menden-Deuer, S., and E. J. Lessard. 2000. Carbon to volume relationships for dinoflagellates, diatoms, and other protist plankton. Limnol. Oceanogr. **45:** 569-579.

Metropolis, N., A. W. Rosenbluth, M. N. Rosenbluth, A. H. Teller, and E. Teller. 1953. Equation of state calculations by fast computing machines. The journal of chemical physics **21:** 1087-1092.

Nishikawa, J., and A. Tsuda. 2001. Feeding of the pelagic tunicate, *Salpa thompsoni*, on flagellates and size-fractionated chlorophyll particles. Plankton biology and ecology **48:** 133-135.

Nordhausen, W., M. Huntley, and M. D. G. Lopez. 1992. RACER: carnivory by *Euphausia superba* during the antarctic winter. Antarctic Journal of the United States **27:** 181-183.

Pakhomov, E. 2000. Demography and life cycle of Antarctic krill, *Euphausia superba*, in the Indian sector of the Southern Ocean: long-term comparison between coastal and open-ocean regions. Canadian Journal of Fisheries and Aquatic Sciences **57:** 68-90.

Pakhomov, E., C. Dubischar, V. Strass, M. Brichta, and U. Bathmann. 2006. The tunicate *Salpa thompsoni* ecology in the Southern Ocean. I. Distribution, biomass, demography and feeding ecophysiology. Mar. Biol. **149:** 609-623.

Pakhomov, E. A., P. W. Froneman, and R. Perissinotto. 2002. Salp/krill interactions in the Southern Ocean: spatial segregation and implications for the carbon flux. Deep-Sea Res. II **49:** 1881-1907. doi: https://doi.org/10.1016/S0967-0645(02)00017-6.

Pakhomov, E. A., and B. P. Hunt. 2017. Trans-Atlantic variability in ecology of the pelagic tunicate *Salpa thompsoni* near the Antarctic Polar Front. Deep-Sea Res. II **138:** 126-140.

Pearce, I., A. T. Davidson, P. G. Thomson, S. Wright, and R. van den Enden. 2011. Marine microbial ecology in the sub-Antarctic Zone: Rates of bacterial and phytoplankton growth and grazing by heterotrophic protists. Deep-Sea Res. II **58:** 2248-2259. doi: 10.1016/j.dsr2.2011.05.030.

Perissinotto, R., E. Pakhomov, C. McQuaid, and P. Froneman. 1997. In situ grazing rates and daily ration of Antarctic krill *Euphausia superba* feeding on phytoplankton at the Antarctic Polar Front and the Marginal Ice Zone. Mar. Ecol. Prog. Ser. **160:** 77-91.

Pfannkuche, O., and K. Lochte. 1993. Open ocean pelago-benthic coupling: cyanobacteria as tracers of sedimenting salp feces. Deep-Sea Res. I **40:** 727-737.

Raskoff, K., F. A Sommer, W. M Hamner, and K. M Cross. 2003. Collection and Culture Techniques for Gelatinous Zooplankton.

Saba, G. K. and others 2014. Winter and spring controls on the summer food web of the coastal West Antarctic Peninsula. Nature Communications **5**. doi: 10.1038/ncomms5318.

Selph, K. E., M. R. Landry, C. B. Allen, A. Calbet, S. Christensen, and R. R. Bidigare. 2001. Microbial community composition and growth dynamics in the Antarctic Polar Front and seasonal ice zone during late spring 1997. Deep-Sea Res. II **48:** 4059-4080. doi: 10.1016/s0967-0645(01)00077-7.

Selph, K. E. and others 2011. Spatially-resolved taxon-specific phytoplankton production and grazing dynamics in relation to iron distributions in the equatorial Pacific between 110 and 140°W. Deep-Sea Res. II **58:** 358-377. doi: 10.1016/j.dsr2.2010.08.014.

Sherr, E. B., and B. F. Sherr. 1994. Bacterivory and Herbivory - Key Roles of Phagotrophic Protists in Pelagic Food Webs. Microbial Ecology **28:** 223-235.

---. 2007. Heterotrophic dinoflagellates: a significant component of microzooplankton biomass and major grazers of diatoms in the sea. Mar. Ecol. Prog. Ser. **352:** 187-197. doi: 10.3354/meps07161.

Silvester, N. 1983. Some hydrodynamic aspects of fitter feeding with rectangular-mesh nets. J. Theor. Biol. **103:** 265-286.

Smith, K. L., Jr. and others 2014. Large salp bloom export from the upper ocean and benthic community response in the abyssal northeast Pacific: Day to week resolution. Limnol. Oceanogr. **59:** 745-757. doi: 10.4319/lo.2014.59.3.0745.

Spiegelhalter, D. J., N. G. Best, B. P. Carlin, and A. Van Der Linde. 2002. Bayesian measures of model complexity and fit. Journal of the royal statistical society: Series b (statistical methodology) **64:** 583-639.

Steinberg, D. K., and M. R. Landry. 2017. Zooplankton and the ocean carbon cycle. Annu. Rev. Mar. Sci. **9:** 413-444.

Stone, J. P., and D. K. Steinberg. 2016. Salp contributions to vertical carbon flux in the Sargasso Sea. Deep-Sea Res. I **113:** 90-100. doi: http://dx.doi.org/10.1016/j.dsr.2016.04.007.

Straile, D. 1997. Gross growth efficiencies of protozoan and metazoan zooplankton and their dependence on food concentration, predator-prey weight ratio, and taxonomic group. Limnol. Oceanogr. **42:** 1375-1385.

Strickland, J. D., and T. R. Parsons. 1972. A practical handbook of seawater analysis, second ed. Bull. Fish. Res. Board Can. **167**.

Stukel, M. R., M. Décima, K. E. Selph, D. A. A. Taniguchi, and M. R. Landry. 2013. The role of *Synechococcus* in vertical flux in the Costa Rica upwelling dome. Prog. Oceanogr. **112-113:** 49-59. doi: 10.1016/j.pocean.2013.04.003.

Sutherland, K. R., L. P. Madin, and R. Stocker. 2010. Filtration of submicrometer particles by pelagic tunicates. Proc. Natl. Acad. Sci. U. S. A. **107:** 15129-15134.

Sutton, P. 2001. Detailed structure of the subtropical front over Chatham Rise, east of New Zealand. J. Geophys. Res. Oceans **106:** 31045-31056.

Taniguchi, D. A. A., M. R. Landry, P. J. S. Franks, and K. E. Selph. 2014. Size-specific growth and grazing rates for picophytoplankton in coastal and oceanic regions of the eastern Pacific. Mar. Ecol. Prog. Ser. **509:** 87-101. doi: 10.3354/meps10895.

Thompson, H. 1948. Pelagic tunicates of Australia. Commonwealth Council for Scientific and Industrial Research.

von Harbou, L., C. D. Dubischar, E. A. Pakhomov, B. P. Hunt, W. Hagen, and U. V. Bathmann. 2011. Salps in the Lazarev Sea, Southern Ocean: I. Feeding dynamics. Mar. Biol. **158:** 2009-2026.

Zeldis, J. R., C. S. Davis, M. R. James, S. L. Ballara, W. E. Booth, and F. H. Chang. 1995. Salp grazing: effects on phytoplankton abundance, vertical distribution and taxonomic composition in a coastal habitat. Mar. Ecol. Prog. Ser.**:** 267-283.

Zeldis, J. R., and M. Décima. 2020. Mesozooplankton connect the microbial food web to higher trophic levels and vertical export in the New Zealand Subtropical Convergence Zone. Deep-Sea Res. I **155:** 103146.